This is a repository copy of *Development of a Training Set of Contemporary Salt-Marsh Foraminifera for Late Holocene Sea-Level Reconstructions in southeastern Australia*.

White Rose Research Online URL for this paper:
https://eprints.whiterose.ac.uk/175961/

Version: Published Version

Article:

Development of a Training Set of Contemporary Salt-Marsh Foraminifera for Late Holocene Sea-Level Reconstructions in southeastern Australia

SOPHIE WILLIAMS (iD)

ED GARRETT (iD)

PATRICK MOSS (iD)

REBECCA BARTLETT

ROLAND GEHRELS (iD)

Author affiliations can be found in the back matter of this article

ABSTRACT

We collected contemporary foraminiferal training sets from two salt marshes to enable more precise and accurate proxy historical sea-level reconstructions from southeastern Australia. Combined with an existing training set from Tasmania, this new regional set consists of 112 samples and 16 species of foraminifera, of which 13 are agglutinated. Cluster analyses group the regional training set into a high–elevation cluster, dominated by *Trochamminita salsa*, a mid–elevation cluster, dominated by *Entzia macrescens* and *Trochammina inflata*, and a mid–low elevation cluster dominated by *Miliammina fusca* and tidal-flat species. We develop transfer functions using local and regional training sets and assess their performance. Our resulting site-specific and chosen regional models are capable of predicting sea level with decimetre-scale precision (95% confidence intervals of 0.12–0.22 m). These results are comparable to other examples from around the world. When developing regional training sets, we advocate that the similarity in the environmental settings (particularly salinity) should be assessed as an alternative way of grouping sites, rather than simply using spatial proximity. We compare our findings with global results and conclude that salt marshes along microtidal coasts yield models with the lowest vertical uncertainties. Studies with the lowest uncertainties are located in the western Pacific and the western Atlantic, whereas those from the eastern Atlantic generally have larger tidal ranges and carry larger vertical uncertainties. Our models expand the existing region available for sea-level reconstruction and can be used to generate new late Holocene sea-level reconstructions across southeastern Australia.

1. INTRODUCTION

Proxy-based palaeo sea-level reconstructions usefully complement historical tide-gauge data (Kopp et al. 2016) as they expand our knowledge of sea-level change beyond instrumental records and can be used to validate instrumental records where both overlap. Proxy data are particularly important in the Southern Hemisphere as tide-gauge records are sparse and often short compared to those in the Northern Hemisphere (Holgate et al. 2013). Both proxy and tide-gauge sea-level data have shown that, globally, the 19th to 20th century sea-level acceleration is larger than any acceleration over the preceding 3000 years (Kopp et al. 2016). Proxy records derived from salt-marsh foraminifera in New Zealand and Tasmania have shown that the rise in regional mean sea level in the earlier half of the 20th century may have been anomalously fast in comparison to the global mean (Gehrels et al. 2008; Gehrels et al. 2012). However, the few long tide-gauge records from the region do not show the same early 20th century trends as the proxy records (*e.g.* Gehrels et al. 2012). Compaction has been suggested as a possibility for the discrepancy between the proxy and instrumental data (*e.g.* Grenfell et al. 2012); however, these Southern Hemisphere salt marshes are shallow and are composed of a stratigraphy not very susceptible to compression (Brain et al. 2012). Therefore, this possible discrepancy is still unexplained.

An important first step towards increasing our understanding of long-term sea-level fluctuations is to develop salt marsh sea-level transfer function models from training sets of contemporary salt-marsh micro-organisms (*e.g.* foraminifera and diatoms; Barlow et al. 2013; Kemp & Telford, 2015). This involves quantifying the relationship between elevation and contemporary foraminifera in order to generate palaeomarsh surface elevations. While there are numerous Northern Hemisphere high-resolution salt marsh sea-level reconstructions based on such microfossil proxies, especially from the North Atlantic region (*e.g.* Barlow et al. 2013; Barnett et al. 2019; Gehrels et al. 2020; Kemp et al. 2017b; 2018; Kopp et al. 2015; 2016; Saher et al. 2015), there are very few from the Southern Hemisphere. High-resolution reconstructions are available for Tasmania (Gehrels et al. 2012), New Zealand (Gehrels et al. 2008; Grenfell et al. 2012), South America (Frederikse et al. 2021) and South Africa (Strachan et al. 2014). However, the potential for salt-marsh based sea-level reconstructions from South Africa, Asia and South America are spatially constrained by the small availability of marsh in these parts of the world, with much greater availability in the Northern Hemisphere (FitzGerald & Hughes, 2019).

Nonetheless, these Southern Hemisphere records are crucial for answering questions about the apparent early 20th century discrepancy in rates of sea-level rise observed between proxy and tide-gauge records (Gehrels et al. 2012; Grenfell et al. 2012), as well as helping to determine the cause of the rapid rise in sea level observed in these records. Gehrels et al. (2012) suggest that the sea-level acceleration observed in the Tasmanian proxy record may be due to the melting of Arctic and Greenland land-based ice, which, as sea-level fingerprinting demonstrates, would result in sea-level rises around Australia (Fleming et al. 2012). Whilst mass loss from the West Antarctic Ice Sheet could also result in sea-level rises along the southeast coast of Australia (Fleming et al. 2012; Gomez et al. 2010), the timing of the apparent sea-level acceleration in the Australian and New Zealand records appears to correspond with a period of anomalous warming in the Arctic (Hegerl et al. 2018) and subsequent enhanced melt of Arctic glaciers and the Greenland ice sheet (*e.g.* Bjørk et al. 2012; Kjeldsen et al. 2015; Parkes & Marzeion, 2018; Vermassen et al. 2020).

It is well established globally that foraminifera occupy specific niches within the tidal frame which reflect both frequency and duration of tidal inundation (*e.g.* Birks, 1995; Gehrels et al. 2012; Kemp et al. 2012; Scott & Medioli, 1978). As such, modern training sets linking salt-marsh elevation with species assemblages can be used to generate transfer functions for empirically-based numerical estimates of past sea-level change when applied to fossil counterparts in cores (Kemp & Telford, 2015; Sachs, Webb & Clark, 1977). In Australia and New Zealand, studies using transfer functions originating from salt-marsh foraminifera have demonstrated their use as a successful proxy, able to predict sea level with sub-decimetre vertical uncertainties (*e.g.* Callard et al. 2011; Grenfell et al. 2012; Southall, Gehrels, & Hayward, 2006). In this paper we develop new local and regional training sets of contemporary salt-marsh foraminifera for southeastern Australia by collecting new samples from Tasmania and New South Wales and combining these with published training sets from Tasmania (Callard et al. 2011). We compare our findings with other microfossil training sets from around the world and assess how transfer function performance is affected by mean tidal range. The training sets presented in this study can be used to establish more salt-marsh based sea-level reconstructions across a wider region in southeastern Australia.

2. STUDY SITES

Existing foraminifera-based training sets from Australia primarily focus on mangrove sediments in the lower latitudes (*e.g.* Haslett, 2001; Horton et al. 2003; Woodroffe et al. 2005); however, sea-level reconstructions from mangrove environments are limited by the dynamic nature of the mangrove ecosystem. Reworking of material is often a large concern, preservation of foraminifera can be poor, and calcareous intertidal foraminifera

with large elevational tolerances can increase vertical uncertainties of transfer function models (Woodroffe, 2009). Salt marshes provide an alternative to mangrove environments for developing modern microfossil training sets and subsequent sea-level reconstructions. Salt marshes are less susceptible to reworking and can often provide sea-level records with centennial to decadal temporal resolution (Gehrels et al. 2012).

We establish new training sets using data collected from a total of four transects at Lutregala salt marsh in the south-west of Tasmania (43.299°S, 147.307°E) and Wapengo salt marsh located in southern New South Wales (36.593°S, 150.009°E) (*Figure 1*). We also employ the previously published foraminiferal training set from Little Swanport, Tasmania (Callard et al. 2011; 42.341°S, 147.931°E). The new sites have minimal evidence of anthropogenic disturbance, are located in bedrock-framed inlets, and have small tidal ranges (≤1 m, see section 3.2). These factors are important to maximise the likelihood that tidal ranges have not changed significantly over time, as this could have affected the vertical foraminiferal zonation. We give site descriptions for the two new sites; site details for Little Swanport can be found in Callard et al. (2011), Gehrels et al. (2012) and Moss, Gehrels & Callard (2016).

2.1 LUTREGALA

Lutregala salt marsh is located on Bruny Island (Indigenous name is lunawanna-allonah) which lies off the coast of Tasmania (lutruwita), around 70 km south-west of Hobart (nipaluna; *Figure 1b*). An isthmus called 'The Neck' joins North and South Bruny Island, with Lutregala, ~0.4 km^2 in area, fronting onto Simpsons Bay on South Bruny Island (Prahalad & Jones, 2013). Due to its sheltered and shallow nature, Simpsons Bay includes several wetland areas (Clark, Cochran & Mazengarb, 2011). The bay is joined to the D'Entrecasteaux Channel, which is located between Bruny Island and mainland Tasmania. The average salinity in Simpsons Bay changes very little annually, with a mean salinity of 32.8 ppt in the bay (Crawford & Mitchell, 1999) and 31.5–34.7 ppt in the surrounding D'Entrecasteaux Channel (Parsons, 2012). The mean nearshore water temperature is 13.88°C (Crawford & Mitchell, 1999). At the northern extent of Lutregala, tidal channels and creeks are prevalent, with three large outflow channels and a system of inflow channels which extend into the salt marsh by several hundred metres. The largest creek, Simpsons Creek, runs through the length of the salt marsh and is part of a larger low-lying saline marsh system supplied by freshwater
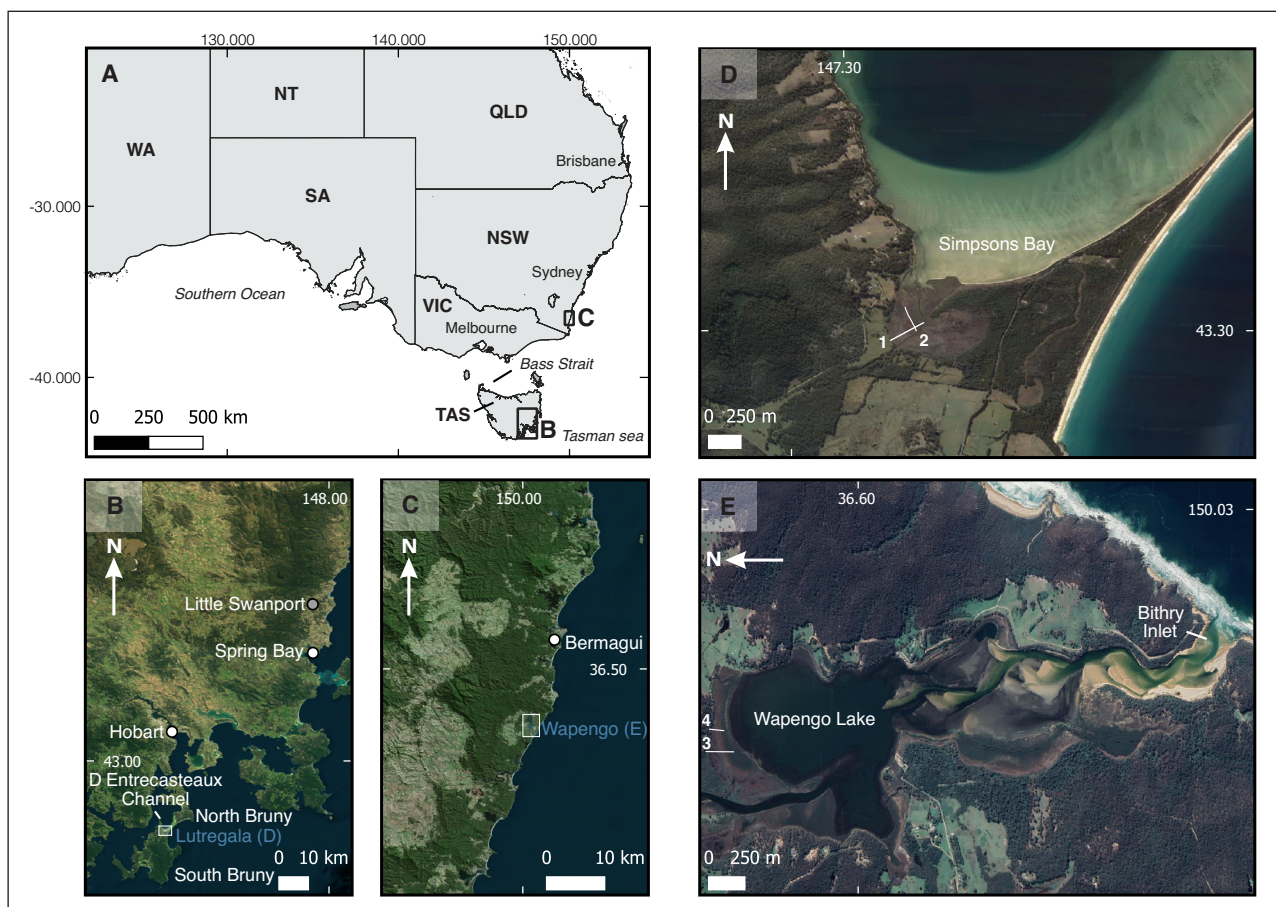
Figure 1 Site and surface transect localities. **A.** Map of Australia detailing state boundaries major cities, seas, oceans and study sites in bounding boxes. **B.** Site and tide-gauge locations (Tasmania), including the previously published site at Little Swanport **C.** Site and tide- gauge location (New South Wales) **D.** Lutregala salt marsh located on Bruny Island, Tasmania. Transects 1 and 2 are surface transects located at Lutregala salt marsh. **E.** Wapengo salt marsh located in southern New South Wales. Transects 3 and 4 are surface transects located at Wapengo salt marsh.

originating in the South Bruny Range (Bryant, 2018). The site and immediate surroundings are underlain by sub- and supra-littoral Quaternary deposits, as well as Quaternary alluvium, aeolian dunes, and sheet sand deposits, and is surrounded by Triassic sandstone and Jurassic Dolerite to the northwest and Permian mudstone formations to the southeast (Farmer & Forsyth 1993).

At Lutregala, the upland is dominated by regenerating grazing land and sclerophyll forest, consisting primarily of *Eucalyptus ovata* (black gum) dry forest with a grassy understorey. There is a patch of *Eucalyptus amygdalina* (coastal black peppermint) forest and *E. ovata* dry forest located on a dune system at the Simpson Bay beach side of the salt marsh (northeast area); we define this as vegetation zone 1 (Z1). Whilst all flora is found throughout the salt marsh, the dominance of the plants vary. The start of the transect 1 is largely characterised by *Juncus krausii* (salt-marsh rush) and *Gahnia filum* (chaffy saw sedge). From 120 m of transect 1, *Sarcocornia quinqueflora* (beaded glasswort) dominates. *Juncus krausii* is absent from 155 m along transect 1; however, all other marsh flora are found until the end of the transect. We define this as vegetation zone 2 (Z2). Along transect 2, all of the dominant marsh flora are found along the length of the transect, but *S. quinqueflora* tends to dominate the start of the transect and *J. krausii* and *G. filum* dominate the lower end of the transect. We note the low abundance of *Tecticornia arbuscula*, (shrubby glasswort), *Samolus repens* (sea primrose) and *Suaeda australis* (seablite) in the salt marsh.

2.2. WAPENGO
Wapengo salt marsh is located around 30 km south of Bermagui in southern New South Wales (***Figure 1c***). The salt marsh, which is around 0.51 km^2 in extent (Creese et al. 2009), is located at the northern end of the Wapengo Lake estuary. Towards the southern end, the estuary has a narrow bedrock-framed mouth (Bithry Inlet). The bottom of the channel is 1.2 m below mean high tide (Roper et al. 2011) and is not fast flowing (Scammell, Batley & Brockbank, 1991). Whilst some sites along this coastline are occasionally cut off from the open ocean, the entrance to Wapengo is permanently open (Scanes et al. 2007), and so Wapengo continuously maintains a connection to the ocean. Due to the proximity to the Bithry Inlet, the site has a high salinity, with multiple recordings from 2010–2012 showing salinity in the range of ~34–37 ppt (Garside et al. 2014). The average temperature in the estuary is ~16°C (Garside et al. 2014). The underlying geology of Wapengo is a formation known as the Adaminaby Group, which comprises Late Ordovician turbidities of metagreywacke and phyllite (Rickard & Love, 2000).

The floral composition at Wapengo salt marsh is similar to that of Lutregala, reflecting the low floral diversity found in the salt marshes of southeastern Australia (Kelleway et al. 2017). We note the presence of a *Eucalyptus sieberi* (stringybark) dry forest with a shrub understorey, which transitions into a narrow fringe of coastal *Melaleuca* (tea tree) forest just above the salt marsh. We define this as vegetation zone 1 (Z1). *Sarcocornia quinqueflora* is most dominant at the start of the transects and declines in dominance down transect, and *J. kraussii* is dominant at the start and end of the transects with a decline in the middle of the salt marsh. *Gahnia filum* is present sporadically at the start, but increases in abundance down transect and is dominant towards the end of the salt marsh. *Tecticornia arbuscula* and *Distichlis distichophylla* (Australian salt grass) also increase in abundance down transect. We also note the low presence of *S. australis* and *Disphyma crassifolium* (rounded-leaved pigface) in the salt marsh. We define this zone of salt-marsh plants as vegetation zone 2 (Z2). A transitional zone sees the appearance of *Avicennia marina* (grey mangrove) interspersed with *T. arbuscula* and *D. distichophylla* which we define as vegetation zone 3 (Z3). This develops into a dense mangrove forest at the lower elevations (vegetation zone 4; Z4).

3. METHODS
3.1 FIELD SAMPLING
We established two transects at each site from upland to tidal flat to obtain samples from all of the ecological zones observed in each salt marsh. At the sampling locations we collected samples ~1 cm in thickness and 12.5 cm^3 in volume.

3.2 ELEVATION AND TIDAL DATA
To enable inter-site comparison, we first related the height of all samples to the Australian Height Datum – Geocentric Datum 2020 (AHD). We established sample elevations using both a Trimble M1 (DR2") total station and a Trimble R4 real-time kinematic GPS relative to a temporary benchmark. To survey sample heights into the geodetic datum, we employed a 'rapid static' method between the temporary benchmark and a local geodetic benchmark. Mean sea level (MSL) and highest astronomical tide (HAT) were obtained from the Australian National Tide Tables (AHP11; Australian Government, Department of Defence, 2020) using data from the nearest local tide station to each site (***Table 1***). As the tide gauges are located 20–50 km from the salt marshes, we checked for spatial differences in tidal range using the TPXO8-Atlas global tidal model (Egbert & Erofeeva, 2010). The tidal range at the Hobart tide gauge is 0.81 m (Australian Government, Department of Defence, 2020) and the TPXO8-Atlas global tidal model indicates a minor difference in tides (0.02 m difference in MSL – HAT

SITE	LOCAL TIDE STATION	MEAN SEA LEVEL (M AHD)	HIGHEST OCCURRENCE OF FORAMINIFERA (HOF) (M AHD)
Lutregala	Hobart	0.05	0.96
Wapengo	Bermagui	–0.03	1.07
Little Swanport	Spring Bay	0.04	0.76

Table 1 Tidal data used to calculate Standardised Water-Level Index (SWLI) values.

range) between the tide gauge and Lutregala (Egbert & Erofeeva, 2010). The tidal range at the Bermagui tide gauge is 1.01 m (Australian Government, Department of Defence, 2020) and the TPXO8-Atlas global tidal model indicates no difference in tidal range between the tide gauge and the entrance to Wapengo Lake estuary (Egbert & Erofeeva, 2010). We normalise tidal range between sites using a Standardised Water-Level Index (SWLI; Zong & Horton, 1999). Wright, Edwards & van de Plassche, (2011) suggest using the highest occurrence of foraminifera (HOF) as the upper datum, as non-linearity between elevation and tidal inundation is most pronounced in the high marsh. Therefore, we applied the following equation:

$$SWLI_n = \frac{100(h_n - h_{MSL})}{h_{HOF} - h_{MSL}} + 100$$

Where $SWLI_n$ is the Standardised Water-Level Index for sample n, h_n is the sample elevation, h_{MSL} is the elevation of mean sea level (MSL), and h_{HOF} is the elevation of the HOF. A SWLI of 100 is MSL and the HOF is 200.

3.3 LABORATORY PROCESSING OF FORAMINIFERAL SAMPLES

Prior to analysis, samples were kept refrigerated below 4°C (Edwards & Wright, 2015). A volume of 5 cm³ of each surface sample was subsampled using a scalpel to remove sediment from the surface sample and a graduated cylinder to measure volume. Samples were shipped to the University of York and stained immediately upon arrival using a buffered solution of rose Bengal and ethanol for 24 hours to distinguish between live and dead specimens (Walton, 1952). Most studies typically stain within 24 hours of collection (*e.g.* Shaw et al. 2016); however, experiments have shown that even after death, foraminiferal protoplasm can stain over a month after collection (Murray & Bowser, 2000). Subsequently, samples were sieved through 500 μm and 63 μm sieves, and the residue from the 63 μm sieve was collected for foraminiferal analyses. Samples were preserved in a solution of deionised water and 30% ethanol until analysis.

As sample counts of ~50–200 are sufficient for low diversity assemblages typical of salt-marsh environments (Edwards & Wright, 2015; Fatela & Taborda, 2002; Grenfell et al. 2012; Kemp, Wright & Cahill, 2020), samples were split into eight equal aliquots using a wet splitter (Scott

& Hermelin 1993). Samples were counted wet via light microscopy using a Zeiss Stemi DV4 microscope at 80×–320× magnification and identified with reference to Hayward, Le Coze & Gross (2019). We retain taxonomic consistency between this training set and the Callard et al. (2011) training set, identifying *Trochamminita* as two distinct species: *Trochamminita salsa* and *Trochamminita irregularis*. The dead assemblage was enumerated, as dead foraminifera have been shown to be a better analogue for fossil assemblages compared to living. This is due to the fact that dead assemblages are independent of factors such as seasonality, minimise temporal variability in modern distributions and are less likely to result in taphonomic bias arising from the dissolution of certain, usually calcareous, species (*e.g.* Grenfell et al. 2012; Horton & Edwards, 2006; Horton & Murray, 2006; Wright, Edwards & van de Plassche, 2011; Walker et al. 2020). Where possible, a count of at least 200 individuals per sample was taken (*e.g.* Chen et al. 2020; Figueira & Hayward, 2014); however, where counts were less than 200, the entire sample was counted.

3.4 TRAINING SET SCREENING

We create transfer function models employing only agglutinated foraminifera following Edwards & Horton (2000). Prior to statistical analyses we removed calcareous species from the training sets (*Quinqueloculia* sp., *Haynesina germanica*, and *Elphidium* sp.) as these species are susceptible to dissolution and are rarely preserved within the fossil salt-marsh sediments (*e.g.* Milker et al. 2015b). Calcareous species totalled 159 out of 27,390 individuals (~0.6% of the combined training set), 157 of which came from Little Swanport (Callard et al. 2011). We also removed samples with total count sizes less than 50 as we deem these statistically unreliable (Kemp, Wright & Cahill, 2020).

3.5 CLUSTERING AND ORDINATION

We employ partitioning around medoids (PAM) clustering and silhouette analysis (Rousseeuw, 1987; Kaufman & Rousseeuw, 1990) to determine biozones present within the training sets using the '*cluster*' (Maechler et al. 2013) and '*Factoextra*' (Kassambara & Mundt, 2017) packages in statistical software R (R Core Team, 2020). We only analyse species distributions against elevation, as this is largely considered to be the environmental variable most responsible for influencing species distributions (*e.g.* Horton et al. 2003; Horton & Murray, 2007; Shaw

et al. 2016). We favour PAM over alternative hierarchical clustering methods, such as k-means, as it is considered more statistically robust (Kemp et al. 2012). The PAM method minimizes a sum of dissimilarities which means there is no requirement for clusters to have a certain size and structure (Chen et al. 2020; Kaufman & Rousseeuw, 1990; Kemp et al. 2012). We determine the optimal number of clusters using the average silhouette method, where a silhouette width (Si) of 1 indicates a sample to be perfectly assigned to the cluster, while –1 indicates incorrect assignment (Kaufman & Rousseeuw, 1990).

We also perform detrended correspondence analysis (DCA; Hill & Gauch, 1980) on the training sets using R packages '*vegan*' (Oksanen et al. 2007) and *cluster*. Ordination plots provide further information on groupings within a training set and have typically been used to show difference and similarity amongst samples. The plots indicate which samples contain higher or lower abundances of certain species based on their distribution around the species' centroid (ter Braak & Verdonschot, 1995). Samples with similar composition are located close together in ordination space, whereas those with dissimilar compositions will plot further away from each other on the ordination plot (Kemp, Horton & Culver, 2009).

3.6 TRANSFER FUNCTION DEVELOPMENT

In previous sea-level reconstruction studies, transfer functions have typically been applied using training sets of data local (*i.e.* within a few kilometres) to the fossil record. However, many studies have advocated for combining training sets from a broad region (*i.e.* from hundreds of kilometres; *e.g.* Barlow et al. 2013; Gehrels, Roe & Charman, 2001; Hocking, Garrett & Cisternas, 2017; Watcham, Shennan & Barlow, 2013; Wilson & Lamb, 2012) to generate regional training sets. Some studies have also sub-divided regional training sets into sub-regional training sets by grouping training sets from sites located in fairly close spatial proximity (*e.g.* Hocking, Garrett & Cisternas, 2017). These studies highlight that whilst the precision of the resulting models often decreases, accuracy increases by providing more modern analogues for the fossil assemblages in cores. We create training sets at varying spatial scales from local up to regional in order to assess how both accuracy and precision alter with increased spatial extent.

To investigate whether the relationship between foraminiferal assemblage and elevation is unimodal or linear, we employ detrended canonical correspondence analysis (DCCA) in CANOCO version 4.5 (ter Braak & Smilauer, 2002). Following Birks (1995), we assume that axis one gradients greater than two standard deviations indicate that species respond unimodally to elevation. Based on the DCCA result, we use either Partial Least Squares (PLS) or Weighted Averaging Partial Least Squares (WAPLS; ter Braak & Juggins, 1993; ter Braak et al. 1993) regression models in R package '*Rioja*' (Juggins, 2020).

Following guidelines from Barlow et al. (2013) and Kemp & Telford (2015) we employ a 'minimum adequate model' approach where no more than three components are used to avoid over-fitting data, and we use the 5% improvement in root-mean-squared-error-of-predictions (RMSEP) rule as guidelines for the use of additional components. We assess transfer function performance via cross-validated model statistics. Bootstrapping is chosen as our cross-validation method because it provides sample-specific errors (ter Braak & Juggins, 1993). In line with the recommendations of Kemp & Telford (2015), we limit outlier removal to a single pass to leave as much natural variability in the models as possible. We consider removing samples with cross-validated residuals exceeding two standard deviations from the mean (Juggins & Birks, 2012). We calculate species optima and tolerances using the R package '*palaeoSig*' (Telford, 2011).

4. RESULTS
4.1 MODERN FORAMINIFERAL DISTRIBUTIONS
4.1.1 Lutregala
At Lutregala, transect 1 spanned a distance of 315 m and transect 2 spanned 260 m. Combined, they covered a vertical range of 0.77 m. A total of 51 surface samples were taken. Within the Lutregala training set, we identified 10 agglutinated species and 1 calcareous species (*Ammonia beccarii* – 1 single individual encountered in the training set). Eleven surface samples had total counts lower than 50 individuals (**Figure 2**); therefore, we removed these samples from the training set. In the resulting training set, the total individual count ranged from 56–814, with an average total count of 232 individuals per sample.

Along transect 1, the HOF was observed at 0.96 m AHD (0.91 m above MSL)**.** Immediately below HOF, the higher elevation samples were dominated by *T. salsa* and *Haplophragmoides wilberti* (0–75% and 0–43% respectively). Mid-low elevations were dominated by *Trochammina inflata* (1–84%), *Entzia macrescens* (0–71%) and *T. irregularis* (0–38%). Low elevation samples were dominated by *Miliammina fusca* (0–97%), with the largest abundance found in the lowest elevation sample. Along transect 2, *E. macrescens* and *T. inflata* dominated the high-mid elevation samples (0–66% and 12–69% respectively). *Trochamminita irregularis and H. wilberti* were also found in these samples at lower abundance (0–13% and 0–16% respectively). Low elevation samples were again dominated by *M. fusca* (0–75%) and, similarly to transect 1, the largest abundance was found in the lowest elevation sample. Minor species included *Siphotrochammina lobata*, *Polysaccammina ipohalina*, *Ammobaculites agglutinans* and *Textularia* sp., which each contribute less than 10% to a sample when present.
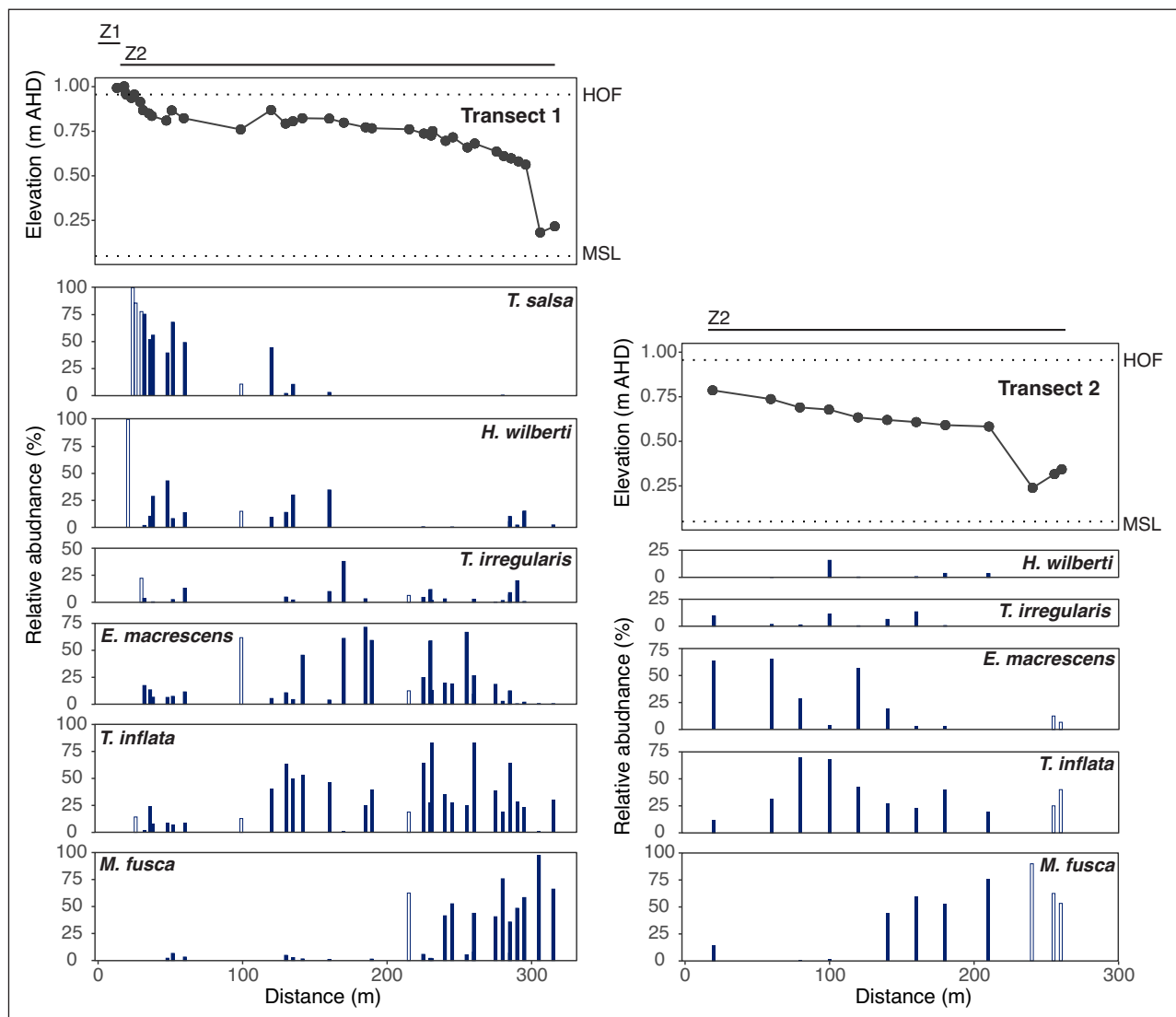
Figure 2 Lateral distribution of surface foraminifera (dead assemblage) along transects 1 and 2 at Lutregala salt marsh. Foraminifera presented represent at least 10% of the total count in at least one sample. Unfilled bars represent total counts lower than 50. The highest occurrence of foraminifera (HOF) was found at 0.96 m AHD (0.91 m above MSL). Vegetation zones are also shown.

4.1.2 Wapengo

At Wapengo, a total of 45 samples were taken. Transect 3 spanned 250 m and transect 4 spanned 60 m. The two surface transects had a total vertical range of 0.71 m. Thirty samples contained total counts greater than 50 (*Figure 3*). Within the resulting training set, we identified 13 agglutinated and 1 calcareous species (*Haynesina germanica* – 1 individual noted within the training set). In the training set, the total count ranged from 55–453 and averages 159 individuals per sample.

The HOF was observed at 1.07 m AHD (1.10 m above MSL). Along transect 3, the high-mid elevation samples were dominated by *T. inflata* and *E. macrescens* (0–92% and 0–55% respectively) with low relative abundances of *T. salsa* (0–2%), *H. wilberti* (0–9%) and *T. irregularis* (0–5%). These samples generally had the lowest total counts (<100 individuals). Mid-elevation samples were dominated by *P. ipohalina* (0–71%) and low elevation samples were dominated by *M. fusca* and *Ammobaculites exiguus* (0–90% and 0–49%) with *A. agglutinans* and

Polysaccammina hyperhalina in low abundance (0–7% and 0–9% respectively). Along transect 4, the high-mid elevation samples were largely dominated by *T. inflata* (0–89%), with a low abundance of *T. salsa* (0–5%) and *Miliammina fusca* (0–72%). *Entzia macrescens* was dominant in the lowest elevation samples (6–85%), with a low abundance of *P. ipohalina* (0–17%). *Siphotrochammina lobata* was also observed in the training set but contributes less than 10% to a sample when present.

4.2 MULTIVARIATE ANALYSES

4.2.1 Partitioning Around Medoids Analysis

Combining samples from Lutregala, Wapengo, and the previously published site at Little Swanport (Callard et al. 2011) into a regional training set, we find that PAM analysis groups samples into three clusters (*Figure 4*). PAM identifies a high-elevation cluster (cluster one), a mid-elevation cluster (cluster two) and a mid-low elevation cluster (cluster three). Cluster one (191 SWLI
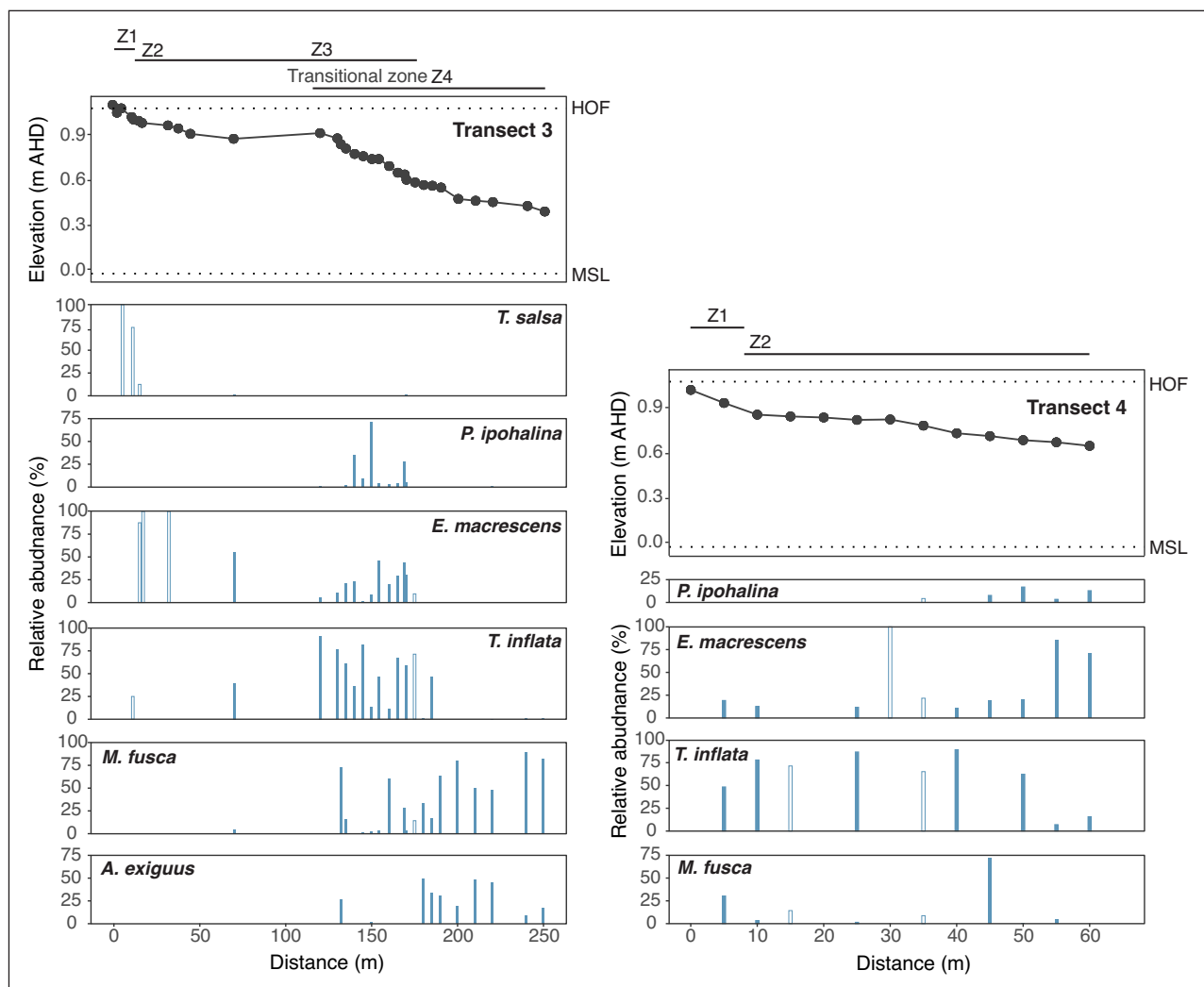
Figure 3 Lateral distribution of surface foraminifera (dead assemblage) along transects 3 and 4 at Wapengo salt marsh. Foraminifera presented represent at least 10% of the total count in at least two samples and filled bars represent counts greater than 50. The highest occurrence of foraminifera (HOF) was found at 1.07 m AHD (1.10 m above MSL). Vegetation zones are also shown.

average) contains large relative abundances of *T. salsa* (average relative abundance 63%); the species is principally dominant at the uppermost elevations, but is present from ~200–155 SWLI. Cluster one also contains the largest relative abundance of *H. wilberti* (~188–156 SWLI; 11% average). Cluster two (163 SWLI average) comprises the majority of samples and is largely composed of *T. inflata* (~200–118 SWLI; 55% average relative abundance) and *E. macrescens* (~190–118 SWLI; 30% average relative abundance). Both species have wide elevational ranges. Cluster three (155 SWLI average) comprises the majority of low elevation samples and has the largest relative abundance of *M. fusca* (average 59%). We find that *M. fusca* is generally sparse at high elevations and increases at lower elevations, with a maximum abundance at 114 SWLI. The cluster also contains typical low-marsh species including *A. exiguus*, *A. agglutinans*, *P. hyperhalina* and *Ammobaculites subcatenulatus*. No samples from Little Swanport were classified into cluster three. This is likely due to the near-absence of *M. fusca* at the site.
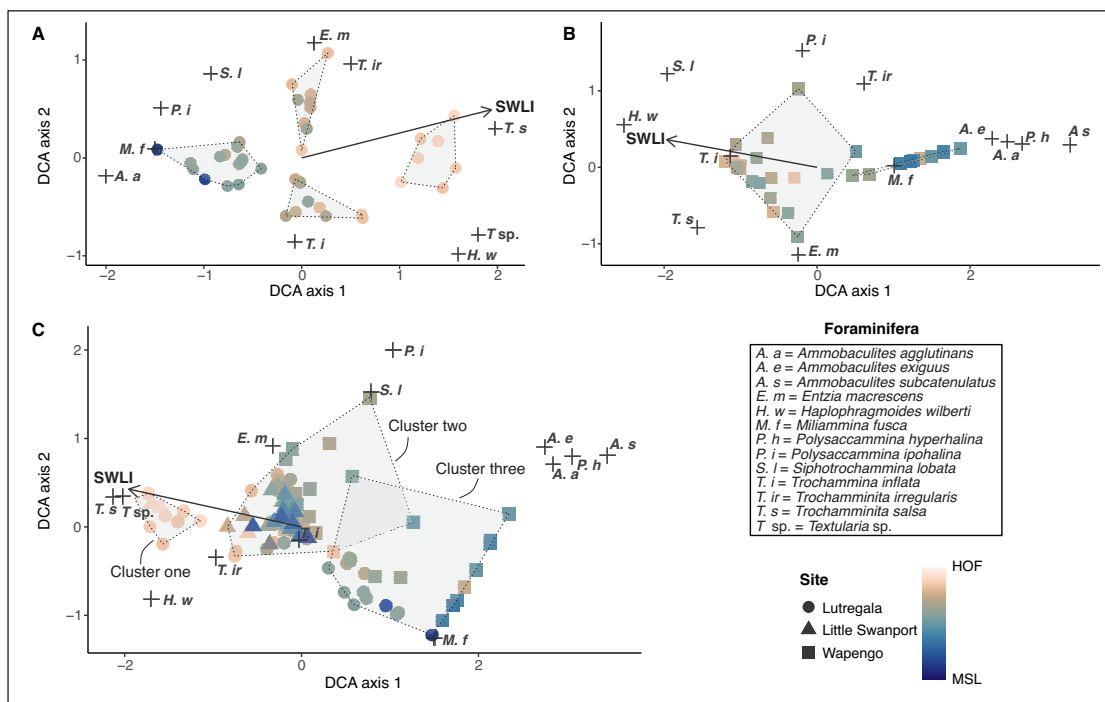
4.2.2 Detrended Correspondence Analysis

DCA analyses (Table S1) indicate that, across all training sets, SWLI is closely aligned with axis 1, although r^2 decreases when samples are combined together with Little Swanport in the regional training set (Lutregala r^2 = 0.60, p = <0.01; Wapengo r^2 = 0.52, p = <0.01; Regional r^2 = 0.22, p = <0.01; *Figure 5*). In each ordination plot, high-elevation samples plot furthest away in ordination space from low-elevation samples, suggesting these samples have the most disparate assemblages.

In the Lutregala training set, four clusters are identified – a high-elevation cluster is dominated by *T. salsa*, a mid-elevation cluster is dominated by *E. macrescens* and *T. irregularis* and another mid-elevation cluster is dominated by *T. inflata* (*Figure 5a*). A low-elevation cluster is dominated by *M. fusca*, with influences from *A. exiguus* and *P. ipohalina*. Conversely, in the Wapengo training set, there is no defined high-elevation cluster; high-mid elevation samples form one cluster largely dominated by *T. inflata* and *E. macrescens* and low-elevation samples are dominated by *M. fusca* and *Ammobaculites* spp. (*Figure 5b*). This may be due to the low abundance of *T.*
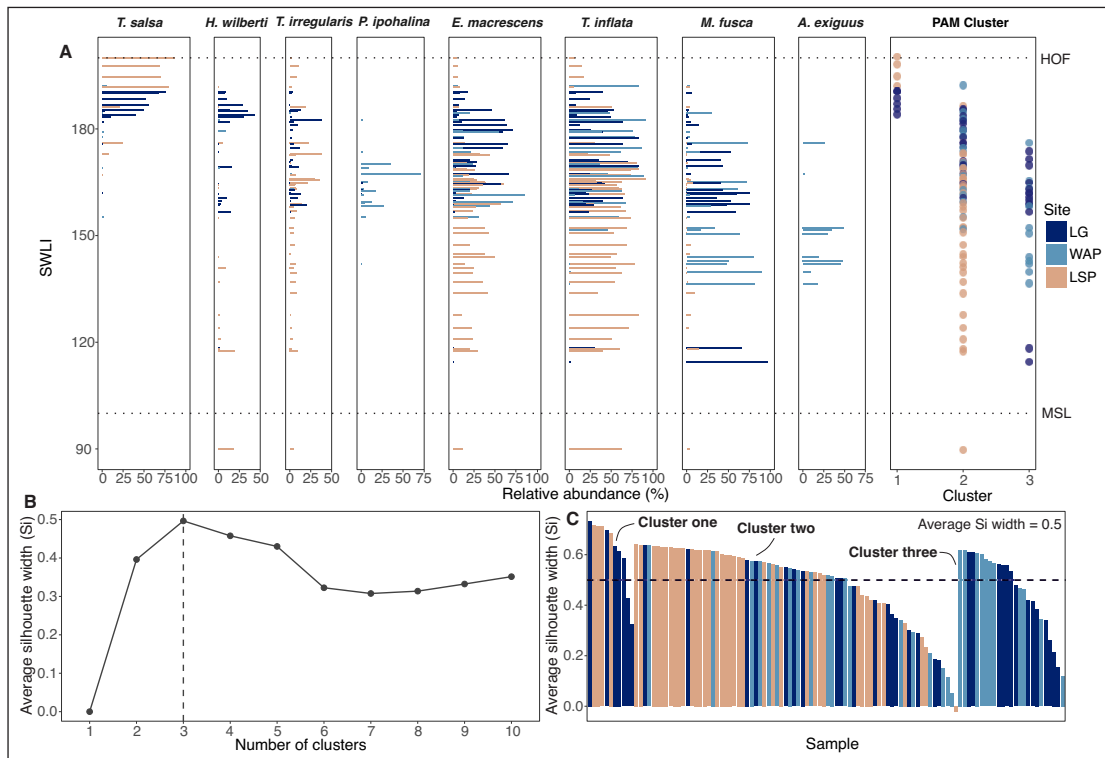
Figure 4 A. Relative abundance of modern foraminifera across the regional training set, showing species exceeding 10% abundance in at least one sample with total counts greater than 50 individuals. Samples are ordered by Standardised Water-Level Index (SWLI); the highest occurrence of foraminifera (HOF) and mean sea level (MSL) are displayed. Partitioning around medoids (PAM) cluster for each sample is shown. **B.** Average silhouette method to determine optimal number of clusters across the regional training set. The peak and the dashed line denotes that samples are best clustered into three groups. **C.** Silhouette width of individual samples within the regional training set. The dashed horizontal line indicates the average silhouette width across the entire regional training set. Site key: LG = Lutregala, WAP = Wapengo, LSP = Little Swanport.

Figure 5 Detrended correspondence analyses of samples from **A.** the Lutregala training set, **B.** the Wapengo training set and **C.** the regional training set (Lutregala, Wapengo and Little Swanport). Cluster number for each detrended correspondence analysis (DCA) plot has been defined by the partitioning around medoids (PAM) algorithm. Samples from varying sites are noted by different symbols. Foraminifera species are denoted by crosses and an associated code. Samples are coloured by Standardised Water-Level Index (SWLI) with samples near mean sea level (MSL; 100 SWLI) in dark blue and samples near highest occurrence of foraminifera (HOF; 200 SWLI) in pink.

salsa at the site (~0–5%), compared with ~50–85% in samples near HOF at Lutregala and Little Swanport.

In the regional training set, cluster one is dominated by *T. salsa* and samples with the highest SWLI values and cluster two is dominated by *T. inflata* and *E. macrescens*, with some influence from *T. irregularis* and *S. lobata* (***Figure 5c***). In cluster three, the mid-low elevation samples towards the centre of the plot are also dominated by *T. inflata* and low-elevation samples are dominated by *M. fusca* and *Ammobaculites* spp. Whilst Little Swanport has low-elevation samples, these samples are grouped into the mid-elevation cluster, again, likely due to the absence of low-marsh and tidal-flat species within the training set. Samples from Lutregala generally plot towards the negative side of the DCA triplot, whereas samples from Wapengo plot to the positive side of the DCA triplot, likely reflecting the differences in species assemblages between the sites, with *T. salsa* near absent from Wapengo but prevalent at Lutregala and *Ammobaculites* spp. and *Polysaccammina* spp. more prevalent at Wapengo but near absent at Lutregala.

4.3 DEVELOPMENT OF A TRANSFER FUNCTION FOR SOUTHEASTERN AUSTRALIA

We develop transfer functions for three local training sets (Lutregala, Wapengo and Little Swanport), a sub-regional training set that comprises the two Tasmanian sites (Lutregala and Little Swanport), a regional training set (I) that includes all samples (Lutregala, Wapengo and Little Swanport), and a regional training set (II) comprising only our new samples (Lutregala and Wapengo). Data are expressed as percentage abundance (***Figure 6***).

Both the Lutregala and Wapengo local training sets, as well as the regional II training set, have axis one lengths greater than two standard deviations (2.05, 2.06 and 2.34 respectively; ***Table 2***) therefore, we apply WAPLS models in these sites. The sub-regional and regional I training sets have axis one lengths less than two standard deviations (1.48 and 1.52 respectively; ***Table 2***); therefore, we apply PLS models. Callard et al. (2011) had previously used a WAPLS and a PLS model on the Little Swanport training set as the axis one gradient length was close to two standard deviations (1.68; ***Table 2***); however, we employ a PLS model (Birks 1995).

The local training sets from Lutregala and Wapengo perform well, with model performance comparable to, or better than, that of the final Little Swanport model reported by Callard et al. (2011) (***Table 3***). The Lutregala model has the lowest RMSEP, demonstrating an ability to predict sea level within ± 6.4 SWLI units (equivalent to ± 0.06 m at Lutregala at 68% confidence or ± 0.12 m at 95% confidence). The Wapengo model prediction error is larger at ± 9.7 SWLI units (equivalent to ± 0.11 m at Wapengo at 68% confidence or ± 0.22 m at 95% confidence). No models exhibit a 5% improvement from component one, therefore we cannot justify the addition of a second component.

Comparison of the sub-regional and regional model I performance with those of the local models highlights that the inclusion of Little Swanport into the models results in a decrease in performance, measured by an increase in RMSEP and a decrease in r^2_{boot} (Sub-regional RMSEP SWLI units = 12.64, r^2_{boot} = 0.41; Regional I RMSEP SWLI units = 12.91, r^2_{boot} = 0.34; ***Table 3***). The residuals are much larger for the sub-regional and regional I model than for the local models, suggesting a poor fit to the observed elevations. Removing Little Swanport from the regional training set (regional II model) results in a ~40% improvement in RMSEP over regional I. Regional II exhibits the best performance of the multi-site models (RMSEP = 7.66 SWLI units, r^2_{boot} = 0.69) and has the second lowest vertical uncertainty after the Lutregala local model (***Table 3***).

We analyse species optima and tolerance across the Lutregala and Wapengo local transfer functions and the regional II transfer function. We find that species optima and tolerances are largely similar between the models (***Figure 7***). The largest discrepancy is in the predicted optima of *M. fusca*; Lutregala and regional II predict the species optima 13 and 6 SWLI units higher respectively than the Wapengo model. We note this pattern is also replicated with *T. salsa*, *T. irregularis* and *E. macrescens*, with higher predicted species optima in the Lutregala and regional II model in comparison to Wapengo. The tolerance of *T. salsa* is also larger in the Wapengo model than in the Lutregala or regional II model. The species with the closest optima between all models is *T. inflata*, with a difference of only 0.95 SWLI units. *Haplophragmoides wilberti* and *P. ipohalina* optima are also predicted at very similar SWLI values across all models (within 1.7 SWLI units or less). The tight vertical optima and tolerance of *P. ipohalina* across all three models highlights the usefulness of this rare species in sea-level reconstruction.

5. DISCUSSION
5.1 CONTROLS ON FORAMINIFERAL DISTRIBUTION AND DIVERSITY

Multivariate analyses demonstrate that elevation (as a proxy for duration and frequency of tidal inundation, or hydroperiod) has an influence on foraminiferal distribution, and supports findings reported across the literature (*e.g.* Avnaim-Katav et al. 2017; Barnett, Garneau & Bernatchez, 2016; Edwards, Wright & van de Plassche, 2004; Gehrels, 2000; Horton & Edwards, 2006; Kemp, Horton & Culver, 2009, Milker et al. 2015a). The ratio of the first constrained DCCA eigenvalue (λ1) to the second unconstrained eigenvalue (λ2) indicates the importance of an environmental variable as a determinant of species distribution (*e.g.* Juggins, 2013). Across all three sites, we find that the ratio exceeds 1
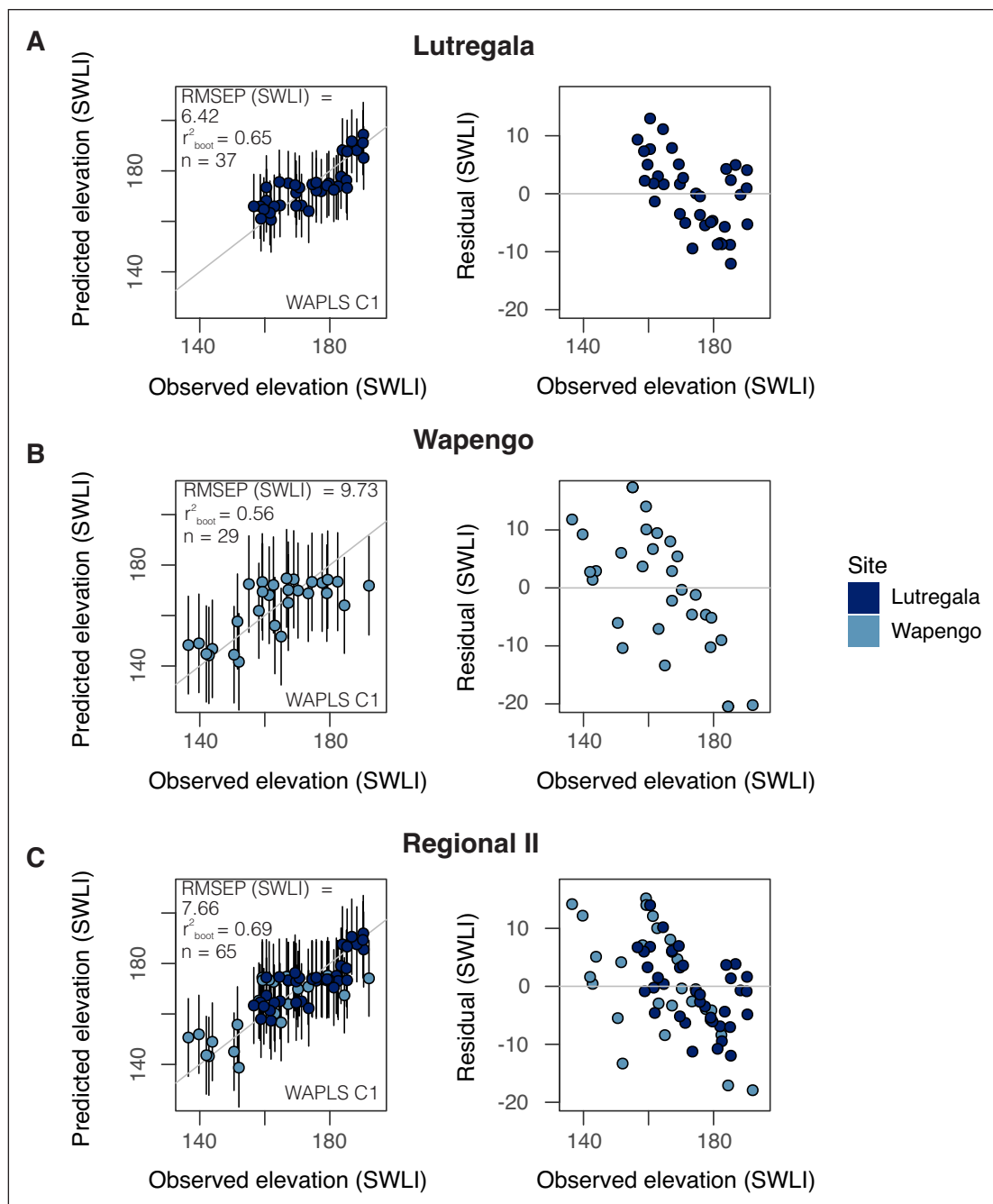
Figure 6 Transfer function performance for local training set models Lutregala **A.** and Wapengo **B.** as well as our chosen regional model **C.** (Lutregala and Wapengo combined). Data are presented with elevation converted to Standardised Water-Level Index (SWLI). 95% prediction uncertainties are given for each sample.

TRAINING SET	AXIS 1 LENGTH	AXIS 1 EIGENVALUE	AXIS 2 EIGENVALUE	AXIS 3 EIGENVALUE	AXIS 4 EIGENVALUE	CUMULATIVE % VARIANCE OF SPECIES DATA	EIGENVALUE ($\lambda 1/\lambda 2$) RATIO
Lutregala	2.05	0.36	0.27	0.15	0.07	24.0	1.33
Wapengo	2.06	0.39	0.30	0.11	0.07	21.7	1.29
Little Swanport	1.68	0.29	0.12	0.05	0.02	28.9	2.51
Sub-regional	1.48	0.19	0.37	0.13	0.09	12.7	0.53
Regional I	1.52	0.19	0.56	0.33	0.16	7.7	0.33
Regional II	2.34	0.39	0.34	0.22	0.13	16.0	1.16

Table 2 Detrended canonical correspondence analysis results for the local, sub-regional and regional training sets.

TRAINING SET	SCALE	SITES INCLUDED IN THE MODEL	NUMBER OF SAMPLES	NUMBER OF SPECIES	MODEL TYPE AND COMPONENT NUMBER	RMSEP (SWLI)	RMSEP (M AHD)	R^2_{BOOT}	AVERAGE BIAS (SWLI)	MAXIMUM BIAS (SWLI)
Lutregala	Local	Lutregala	37	9	**WAPLS C1**	**6.42**	**0.06**	**0.65**	**−0.01**	**7.86**
					WAPLS C2	6.57	0.06	0.65	0.13	7.42
					WAPLS C3	7.40	0.07	0.60	0.14	8.62
Wapengo	Local	Wapengo	29	12	**WAPLS C1**	**9.73**	**0.11**	**0.56**	**0.12**	**20.32**
					WAPLS C2	10.80	0.12	0.53	0.50	18.14
					WAPLS C3	12.49	0.14	0.50	1.02	18.77
Little Swanport	Local	Little Swanport	41	6	**PLS C1**	**15.23**	**0.11**	**0.42**	**0.11**	**32.74**
					PLS C2	15.55	0.11	0.44	−0.03	32.95
					PLS C3	14.88	0.11	0.53	−0.38	28.23
Sub-regional	Sub-regional	Lutregala & Little Swanport	76	9	**PLS C1**	**12.64**	**–**	**0.41**	**0.00**	**32.83**
					PLS C2	12.71	–	0.41	0.11	33.86
					PLS C3	12.91	–	0.40	0.21	33.67
Regional I	Regional	Lutregala, Wapengo & Little Swanport	105	13	**PLS C1**	**12.91**	**–**	**0.34**	**0.06**	**35.12**
					PLS C2	12.40	–	0.36	0.06	34.34
					PLS C3	12.39	–	0.37	0.06	34.68
Regional II	Regional	Lutregala & Wapengo	65	13	**WAPLS C1**	**7.66**	**–**	**0.69**	**0.07**	**9.15**
					WAPLS C2	8.49	–	0.65	0.29	8.54
					WAPLS C3	9.68	–	0.63	0.50	8.18

Table 3 Summary statistics for cleaned model data across local, sub-regional and regional training sets. Rows highlighted in bold indicate the chosen model for each training set.
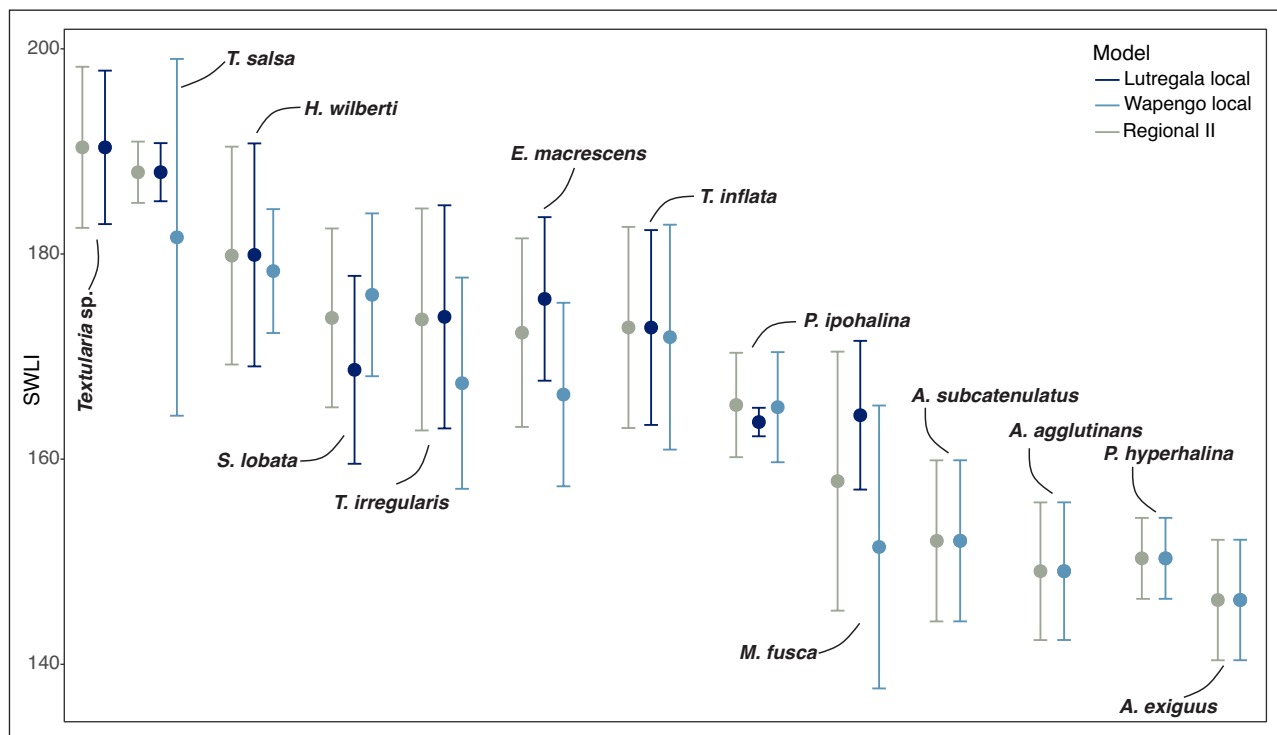
Figure 7 Species optima and tolerances from the local Lutregala and Wapengo models and the regional II model.

(λ1/λ2 = 1.33, 1.29 and 2.51 at Lutregala, Wapengo and Little Swanport respectively; *Table 2*), further suggesting that elevation is an important environmental variable in explaining species distribution at all sites. DCCA axis 1 values suggest elevation is responsible for 24%, 22% and 29% of the cumulative variance of species data at Lutregala, Wapengo and Little Swanport respectively (*Table 2*); however, these values are generally lower than those typically reported in other foraminiferal studies (*e.g.* Hawkes et al. 2010; Horton & Edwards, 2006). Barnett, Garneau & Bernatchez (2016) show that for *M. fusca* and *T. inflata*, some of the most dominant species in our training set, the amount of taxa variation accounted for by axis 1 is low. Furthermore, the values are not out of ranges reported elsewhere in the literature – Avnaim-Katav et al. (2017) report elevation influences 17.1% of species distribution in their training set. Our values may therefore suggest other environmental variables also influence species distribution at the sites.

We find that the vertical distribution of species varies spatially, with foraminifera at Little Swanport having the widest vertical distributions (*Figure 4a*). For example, *H. wilberti*, *T. irregularis* and *E. macrescens* are generally observed at SWLI values above 150 at Lutregala and Wapengo, but are present at 89 SWLI at Little Swanport, a difference of ~61 SWLI units. Freshwater flooding events (Pearce et al. 2005) and variable rainfall (Hedge & Kriwoken, 2000) in the Little Swanport estuary have periodically lowered the salinity in the estuary to values lower than 10 ppt (Crawford & Mitchell, 1999). We suggest this may cause a non-uniform salinity gradient across the salt marsh, which can cause poorly defined vertical distributions (de Rijk & Troelstra, 1997). Low and variable salinity at the site may also explain the low abundance of *M. fusca* site in comparison to Lutregala and Wapengo.

Salinity may also influences species diversity; Wapengo has the highest species diversity, followed by Lutregala. Foraminifera have higher species diversities at salinities of 32–27 ppt (Murray, 2006), and both the Lutregala and Wapengo estuaries have salinity values in this range (Crawford & Mitchell, 1999; Garside et al. 2014; Parsons, 2012). The average salinity in the Little Swanport estuary is ~27 ppt and decreases to ~20 ppt in the salt marsh and mudflat (Sakabe & Lyle, 2010); therefore, the weaker and variable salinity in the Little Swanport estuary may also explain the lower species diversity of this site. The higher species diversity at Wapengo is a result of the presence of a greater number of *Ammobaculites* species. Lal et al. (2020) suggest that high abundances of *Ammobaculites* spp. are correlated with a transition from mangrove to mixed mangrove and salt-marsh vegetation at the mid-elevations of the upper intertidal zone. *Ammobaculites exiguus* has been noted to often reside within mangroves and in unvegetated muddy tidal and sand flats, which we find at Wapengo (Hayward & Hollis, 1994; Schröder-Adams,Boyd & Tran, 2014). Vegetation is influenced by elevation and salinity (Lal et al. 2020); therefore we suggest that a combination of tidal frequency and duration as well as salinity and vegetation type exert influence on species distribution and diversity at our sites.

5.2 FORAMINIFERAL DISTRIBUTIONS AND DIVERSITY IN SOUTHEASTERN AUSTRALIA AND NEW ZEALAND

Modern foraminiferal distributions at Lutregala and Wapengo are broadly similar to those observed in other studies from southeastern Australia and New Zealand. At four sites located near Wollongong, New South Wales, *M. fusca*, *E. macrescens* and *T. inflata* also dominate surface sample assemblages (Lal et al. 2020). *Trochammina inflata* is especially dominant, which is also a common occurrence in New Zealand salt marshes (Hayward, 2014), with the species noted to often be found from pasture and salt meadow to mangroves (Hayward, Grenfell & Scott, 1999).

We find *T. salsa* present from ~155–200 SWLI (the upper half of the range between MSL and HOF), which is broadly similar to previous work conducted in New Zealand, where *T. salsa* is largely found in the upper third of the intertidal zone (Hayward & Hollis, 1994). The species can often extend into the upper reaches of estuaries, and is common in brackish settings with significant freshwater input (Hayward, 2014; Hayward, Grenfell & Scott, 1999; Hayward & Hollis, 1994). The species has previously been noted both in Tasmania (Callard et al. 2011) and Victoria (Apthorpe, 1980), and, in agreement with our findings, often occurs as a near-monospecific fauna (Hayward, 2014). However, the species is not documented in lower latitude Australian sites (Berkeley et al. 2008, 2009; Cann et al. 1993; Haslett, 2001; Haslett et al. 2010; Horton et al. 2003; Lal et al. 2020; Strotz, 2015; Wang & Chappell, 2001; Woodroffe, 2005), which may suggest that the species has a preference for temperate salt marshes in Australia.

Of the dominant agglutinated taxa noted in Lal et al. (2020) (*i.e.* those found at all of their Northern New South Wales sites), which includes *Ammobaculites* spp., *Ammotium directum*, *E. macrescens*, *M. fusca*, *S. lobata* and *T. inflata*, we note the presence of all but *A. directum* in our regional training set. Furthermore, Lal et al. (2020) encounter *H. wilberti*, but do not find it at every site. Previous literature shows *A. exiguus* can tolerate a wider range of salinities, usually around 20–32 ppt (Ostrognay & Haig, 2012; Schröder-Adams, Boyd & Tran, 2014), with preferences for mangrove and tidal flat environments (Hayward & Hollis, 1994; Schröder-Adams, Boyd & Tran, 2014). We find *A. exiguus* in one creek sample at Lutregala, and the species is absent from Little Swanport, supporting evidence of the species' preference for mangrove and muddy substrate.

Rarer species encountered by both Lal et al. (2020) and this study include *Textularia* spp.*,* and *P. ipohalina*. *Polysaccammina ipohalina* is noted to be rare in temperate salt marshes, but has also been documented in New Zealand (Hayward, Grenfell & Scott, 1999). Whilst the species is found both at Lutregala and Wapengo, it is more prevalent at the latter site. *Polysaccammina ipohalina* has

been associated as often subdominant to *E. macrescens* and *T. inflata* environments (Camacho et al. 2015), which is replicated also at our sites.

Haslett et al. (2010) observed modern distributions at Minnamurra Inlet, one of the four sites studied by Lal et al. (2020) and note the presence of *T. inflata, Ammobaculites* spp.*,* and *Haplophragmoides* spp.*,* but also encountered species not found at our sites, with the site reflecting a higher species diversity. However, they find only very low total counts in all surface samples (mean 3.27 specimens/g sediment), with single occurrences common. Furthermore, at Smiths Lake located north of Sydney (Strotz, 2015), species diversity of benthic foraminifera is also markedly higher than at our sites. Species common to our sites include *M. fusca, T. inflata, Textularia* spp.*,* and *A. agglutinans.* We find species diversity tends to be higher at these lower latitude sites as calcareous foraminifera are far more prevalent.

We do not include the samples from Haslett et al. (2010), Lal et al. (2020), and Strotz (2015) in our regional training set due to the site and sample selection criteria outlined in this paper. Lal et al. (2020) employ both living and dead foraminifera in their relative abundance counts, whereas our training set uses only dead assemblages. The Haslett et al. (2010) training set has insufficient total counts (<50 individuals) and the Strotz (2015) training set does not comply with our site selection guidelines, as the training set is derived from an artificially managed system. Other benthic foraminiferal studies from Australia (*i.e.* Berkeley et al. 2008; Cann et al. 1993; Dean & De Deckker, 2013; Haslett, 2001; Horton et al. 2003; Wang & Chappell, 2001; Woodroffe, 2005) are either located outside of the region of interest, lack elevation data, or use grab samples that are not representative of the surface assemblages.

5.3 IMPLICATIONS OF ENVIRONMENTAL VARIABILITY ON REGIONAL TRANSFER FUNCTION PERFORMANCE

Whilst the role of frequency of tidal inundation as a primary driver of the vertical distribution of foraminifera has long been established (*e.g.* Scott & Medioli, 1978), other abiotic and biotic factors such as food availability, oxygen, organic matter, grain size, salinity, vegetation and temperature can also influence species distributions (*e.g.* Murray, 2006). Multivariate analyses of contemporary salt-marsh foraminifera from salt marshes on the Atlantic coast of North America have directly indicated that elevation does not exclusively control foraminiferal distribution (Edwards, Wright & van de Plassche, 2004; Wright, Edwards & van de Plassche, 2011). Whilst regional models can be advantageous due to the fact that they combine sites with differing physiographical and environmental parameters, making them applicable to a larger range of palaeoenvironments (Kemp & Telford, 2015), we find that the differing vertical foraminiferal

distribution between species at Little Swanport and the two new sites greatly affects model performance. In both the sub-regional and regional I transfer functions, nearly all Little Swanport samples have predicted elevations ~158 SWLI (see Figure S1). This is likely due to the near absence of *M. fusca* and dominance of *T. inflata* at the site. As such, while the regional II transfer function is appropriate for reconstructing sea level from fossil assemblages at both Lutregala and Wapengo, this model is likely not suitable for reconstructions at sites with low (*i.e.* less than ~30 ppt) or variable salinity. We suggest that in such cases, a local model is currently more suitable and further modern samples should be collected to extend the training set. In line with other studies (*e.g.* Watcham et al. 2013; Hocking, Garrett & Cisternas, 2017), we suggest that when employing regional models, a wide spatial extent beyond a sub-region may be needed for good model performance.

5.4 THE USE OF TRANSFER-FUNCTION MODELS IN RELATIVE SEA-LEVEL RECONSTRUCTION
5.4.1 Comparison with other local and regional sea-level transfer-function models

Transfer function approaches are now widely employed in palaeoenvironmental research as they provide a quantitative and largely objective method by which reconstructions of palaeoenvironmental conditions can be directly compared and replicated by other studies (Kemp & Telford, 2015). We compare our transfer-function model performance with other proxy-based transfer functions from the literature, updating a global database of transfer function performance versus mean tidal range (MTR; Barlow et al. 2013; Barnett et al. 2017; Callard et al. 2011; Mills et al. 2013). The updated database integrates data from multiple proxies used in sea-level reconstruction: diatoms, benthic foraminifera, testate amoebae and pollen (*Table 4*).

We find a positive and significant correlation between MTR and model performance (both local and regional models) assessed using RMSEP ($r^2 = 0.44$, n = 67, p = <0.01; *Figure 8a*). Our results suggest that microtidal ranges, such as those seen at Lutregala and Wapengo, provide the optimal environments for sea-level reconstructions as they yield models with low vertical uncertainties. We find that, due to generally smaller MTR, sites in the western Pacific (*e.g.* Callard et al. 2011; Horton et al. 2003; Southall, Gehrels & Hayward, 2006), western Atlantic, (*e.g.* Barnett, Garneau & Bernatchez, 2016; Horton et al. 2006; Kemp, Horton & Culver; Wright, Edwards & van de Plassche, 2011) and South Atlantic (*e.g.* Newton et al. 2021), have lower vertical uncertainties, whereas those from the eastern Atlantic, with larger tidal ranges, have larger vertical uncertainties (*e.g.* Barlow et al. 2013; Horton & Edwards, 2005; Massey et al. 2006; Mills et al. 2013). This supports findings previously described in the literature. When our regional model is compared to other

regional models from across the world (*Figure 8b*), we note that our model performs well, with similarly small vertical uncertainties to western Atlantic regional models from Barnett, Garneau & Bernatchez, (2016), Charman et al. (2010), Horton et al. (2006) and Kemp, Horton & Culver, (2009). Spatially, the closest regional training set to ours currently is located in Japan (Sawai, Horton & Nagumo, 2004); most regional training sets come from the East and West Atlantic; therefore, future work should concentrate on developing more training sets for the western Pacific (Oceania) region in order to better resolve recent sea-level histories for this region of the world.

5.4.2. Alternative methods for paleoenvironmental reconstruction

An alternative to the transfer-function approach is a 'visual assessment' (VA; Long et al. 2010). VAs may be used to assess key changes in microfossil taxa, whilst incorporating environmental data. Variables such as stratigraphy, loss on ignition and particle size, which cannot be incorporated into traditional transfer-function analyses, can be considered with a VA approach. VAs may also be used where the modern training set yields no good modern analogues for fossil material (*e.g.* Barnett et al. 2015). This method is not used widely, but may be utilised at sites with microtidal ranges, particularly in the upper marsh where species are mostly constrained to a small vertical range. However, the VA method has been criticised as it considers elevation as a discrete variable which can result in step changes in relative sea-level reconstructions, whereas transfer-function approaches produce sample-specific errors as elevation is treated as a continuous variable (Kemp et al. 2017b). Furthermore, generally, transfer-function approaches will yield models with lower vertical uncertainties (Kemp & Telford, 2015). The recent use of Bayesian transfer functions in relative sea-level reconstruction provides an alternative to both of these methods and may incorporate the best aspects of both approaches (*e.g.* Cahill et al. 2016; Kemp et al. 2017a; Walker et al. 2021). Future relative-sea level studies may choose to use this approach over the more traditional transfer-function method.

6. CONCLUSIONS

This study is the first to collate salt-marsh foraminifera into a regional training set for southeastern Australia and produces new transfer functions that will underpin future late Holocene sea-level reconstructions in the region. We report assemblages from two new sites: Lutregala salt marsh located on Bruny Island, Tasmania and Wapengo salt marsh located in southern New South Wales, and combine these with a previously published training set from Little Swanport, Tasmania (Callard et al. 2011), successfully expanding the available region for

REGION	SITE	REF	MODEL	MICROFOSSIL	N	RMSEP	MTR	RMSEP/MTR
Adriatic	Croatia – Values given relative to Split tide gauge	Shaw et al. (2016)	WA-PLS	Foraminifera	60	0.08	0.19	42.1
Eastern Atlantic	Brancaster Marsh, UK	Gehrels,Roe & Charman, (2001)	WA-Tol	Diatoms	88	0.21	3.81	1.4
Eastern Atlantic	Brancaster Marsh, UK	Gehrels,Roe & Charman, (2001)	PLS	Foraminifera	90	0.08	3.81	2.2
Eastern Atlantic	Brancaster Marsh, UK	Gehrels,Roe & Charman, (2001)	PLS	Testate	52	0.08	3.81	2.2
Eastern Atlantic	UK – Values given relative to Cowpen Marsh	Horton,Edwards & Lloyd, (1999)	WA-Tol	Foraminifera	131	0.12	3.37	3.4
Eastern Atlantic	Mersey River UK	Mills et al. (2013)	WA-PLS	Foraminifera	56	0.13	5.93	2.2
Eastern Atlantic	Ho Bugt Denmark	Szkornik,Gehrels & Kirby, (2006)	WA-PLS	Diatoms	40	0.14	1.5	9.3
Eastern Atlantic	UK- Values given relative to Cowpen Marsh	Zong & Horton, (1999)	WA-Tol	Diatoms	88	0.21	3.37	6.3
Eastern Atlantic	Scotland (average of 9 locations)	Barlow et al. (2013)	WA-PLS	Diatoms	215	0.4	4.3	9.3
Eastern Atlantic	Scotland (average of 9 locations)	Barlow et al. (2013)	WA-PLS	Diatoms	121	0.21	4.3	4.9
Eastern Atlantic	Scotland	Barlow et al. (2013)	WA-PLS	Diatoms	73	0.16	4.3	3.7
Eastern Atlantic	Scotland	Barlow et al. (2013)	WA-PLS	Diatoms	53	0.1	4.3	2.3
Eastern Atlantic	Norway – Values given relative to Lødingen	Barnett, (2013)	WA-PLS	Testate	29	0.09	1.92	4.7
Eastern Atlantic	Western Denmark	Gehrels and Newman, (2004)	WA-Tol	Foraminifera	16	0.16	1.5	10.7
Eastern Atlantic	Florida, USA – Values given relative to Little Manatee River	Gerlach et al., (2017)	WA-PLS	Foraminifera	66	0.07	0.47	14.9
Eastern Atlantic	Bristol Channel, England	Hill et al. (2007)	WA-Tol	Diatoms	61	0.88	11.66	7.5
Eastern Atlantic	Norfolk, England (average of 2 locations)	Horton and Edwards, (2005)	WA-PLS	Foraminifera	47	0.25	4.8	5.2
Eastern Atlantic	Southern Portugal	Leorri et al. (2010)	PLS	Foraminifera	22	0.14	2	7
Eastern Atlantic	Northern Portugal	Leorri et al., (2011)	WA-PLS	Foraminifera	30	0.1	1.95	5.1
Eastern Atlantic	Brittany, France	Leorri et al., (2010)	PLS	Foraminifera	43	0.22	2.59	8.5
Eastern Atlantic	Northern Spain (average of 4 sites)	Leorri, Horton & Cearreta, (2008)	WA-PLS	Foraminifera	30	0.19	2.5	7.6
Eastern Atlantic	South Devon	Massey et al. (2006)	WA-PLS	Foraminifera	85	0.29	4.65	6.2
Eastern Atlantic	Schedlt estuary, Belgium	Ooms, Beyens and Temmerman, (2012)	WA-PLS	Testate	37	0.24	4.98	4.8

(Contd.)

REGION	SITE	REF	MODEL	MICROFOSSIL	N	RMSEP	MTR	RMSEP/MTR
Eastern Atlantic	Brittany, France (average of 2 sites)	Rossi et al., (2011)	PLS	Foraminifera	36	0.07	3	2.3
Eastern Atlantic	Brittany, France – Values given relative to Bay of Brest	Stéphan et al. (2014)	WA-PLS	Foraminifera	29	0.2	3.89	5.1
Eastern Pacific	Upper Cook Inlet, Alaska USA (average of 4 locations)	Barlow,Shennan & Long, (2012)	WA-PLS	Diatoms	149	0.3	7.98	3.8
Eastern Pacific	California, USA – Values given relative to Tijuana River Estuary	Avnaim-Katav et al. (2017)	WA-PLS	Foraminifera	55	0.09	1.13	8.4
Eastern Pacific	Alaska, USA	Hamilton & Shennan, (2005)	WA-PLS	Diatoms	154	0.11	7.98	1.4
Eastern Pacific	Oregon (average of 5 sites)	Hawkes et al., (2010)	WA-PLS	Foraminifera	91	0.2	1.81	11
Eastern Pacific	Chile, South America – Values given relative to Chaihuín	Hocking, Garrett & Cisternas, (2017)	WA-PLS	Diatoms	176	0.23	0.95	24
Eastern Pacific	Southern Oregon – values given relative to South Slough	Milker et al. (2016)	WA-PLS	Diatoms	160	0.16	1.71	9.2
Eastern Pacific	Alaska, USA – Values given relative to Anchorage	Watcham, Shennan and Barlow, (2013)	WA-PLS	Diatoms	255	0.66	8	8.3
Northern Atlantic	Viðarholmi Iceland	Gehrels et al. (2006)	WA-Tol	Foraminifera	21	0.2	2.1	9.5
Northern Atlantic	Viðarholmi Iceland	Saher et al., (2015)	WA-PLS	Diatoms	53	0.09	2.1	4.3
Northern Atlantic	Aasiaat, Greenland	Woodroffe & Long, (2010)	WA-PLS	Diatoms	64	0.16	2.7	5.9
Northern Atlantic	Sisimut, Greenland	Woodroffe& Long (2010)	WA-PLS	Diatoms	70	0.19	4.5	4.2
Red Sea	Shuaiba Lagoon	Abu-Zied & Bantan, (2013)	WA-PLS	Foraminifera	29	0.16	0.06	266.7
South Atlantic	Galpins salt-marsh – Values given relative to Port Elizabeth	Strachan et al. (2015)	PLS	Foraminifera	37	0.17	1.12	15.2
South Atlantic	Swan Inlet	Newton et al. (2021)	WA-Tol	Testate amoebae	28	0.13	0.07	0.19
South Atlantic	Swan Inlet	Newton et al. (2021)	WA-PLS	Diatoms	37	0.06	0.07	0.09
South Atlantic	Swan Inlet	Newton et al. (2021)	WA-PLS	Multiproxy	46	0.09	0.07	0.13

(Contd.)

REGION	SITE	REF	MODEL	MICROFOSSIL	N	RMSEP	MTR	RMSEP/MTR
Western Atlantic	Magdalen Islands – Values given relative to Cap-aux-Meules	Barnett,Garneau & Bernatchez, (2016)	PLS	Foraminifera	39	0.12	0.29	41.4
Western Atlantic	Magdalen Islands	Barnett,Garneau & Bernatchez, (2016)	Wa-Cla	Testate	62	0.08	0.29	27.6
Western Atlantic	Newfoundland	Wright,Edwards & van de Plassche, (2011)	WA-PLS	Foraminifera	37	0.07	0.83	8.4
Western Atlantic	Pattagansett River, Connecticut, USA	Wright,Edwards & van de Plassche, (2011)	WA-PLS	Foraminifera	26	0.1	1.16	8.6
Western Atlantic	Maine and Nova Scotia, North America – Values given relative to the Chezzetook Inlet	Charman et al. (2010)	WA-Tol	Testate	29	0.05	1.25	4.2
Western Atlantic	Connecticut USA (average of 4 sites)	Edwards, Wright & van de Plassche, (2004)	WA-PLS	Foraminifera	91	0.18	1.36	13.2
Western Atlantic	Maine USA (average of 4 sites)	Gehrels, (2000)	WA-PLS	Foraminifera	68	0.25	3.11	8
Western Atlantic	Nova Scotia	(Gehrels et al. 2005)	WA-Tol	Foraminifera	46	0.06	1.86	3.2
Western Atlantic	New Brunswick, Canada	Gehrels, Hendon & Charman, (2006)	WA	Testate	12	0.08	5.8	1.4
Western Atlantic	Maine, USA	Gehrels,Hendon & Charman, (2006)	WA	Testate	17	0.07	2.6	2.7
Western Atlantic	Delaware, USA	Gehrels,Hendon & Charman, (2006)	WA	Testate	9	0.07	1.75	4
Western Atlantic	Outer Banks North Carolina USA (average of 3 sites)	Horton et al. (2006)	WA-PLS	Diatoms	46	0.08	0.35	22.9
Western Atlantic	Outer Banks North Carolina USA (average of 10 sites)	Kemp et al. 2009	WA-PLS	Foraminifera	46	0.04	0.27	14.8
Western Atlantic	New Jersey – Values given relative to Leeds Point	Kemp et al. (2012)	WA-PLS	Foraminifera	62	0.14	1.16	11.8
Western Atlantic	New Jersey – Values given relative to Leeds Point	Kemp et al. (2013)	WA	Foraminifera	175	0.15	1.16	13.2
Western Atlantic	Elizabeth River, North Carolina, USA	Wright, Edwards & van de Plassche, (2011)	WA-PLS	Foraminifera	53	0.14	1.34	10.4
Western Pacific	Kaledupa	Engelhart et al. (2007)	ML	Pollen	63	0.22	1.13	19.6

REGION	SITE	REF	MODEL	MICROFOSSIL	N	RMSEP	MTR	RMSEP/MTR
Western Pacific	Central Great Barrier Reef – values given relative to Cleveland Bay	Horton et al. (2007)	WA-PLS	Foraminifera	43	3.5	1.51	231.1
Western Pacific	Hokkaido Japan (average of 2 sites)	Sawai, Horton & Nagumo, (2004)	WA-PLS	Diatoms	78	0.29	1.05	27.6
Western Pacific	Caitlins Coast	Southall, Gehrels, & Hayward, (2006)	WA-Tol	Foraminifera	31	0.05	1.5	3.3
Western Pacific	Little Swanport	Callard et al. (2011)	WA-PLS	Foraminifera	43	0.1	0.6	16.7
Western Pacific	New Zealand -Values given relative to Mokomoko	Garrett et al. (Unpublished)	PLS	Foraminifera	77	0.08	1.89	4.2
Western Pacific	Manukau Harbour	Grenfell et al. (2012)	WA-Tol	Foraminifera	25	0.11	1.84	6
Western Pacific	Cocoa Creek, Great Barrier Reef Coastline, Australia	Horton et al. (2003)	WA-PLS	Foraminifera	34	0.07	1.48	4.7
Western Pacific	**Lutregala**	**This study**	**WA-PLS**	**Foraminifera**	**37**	**0.06**	**0.47**	**12.8**
Western Pacific	**Wapengo**	**This study**	**WA-PLS**	**Foraminifera**	**28**	**0.11**	**0.95**	**11.6**
Western Pacific	**Regional II – Values given relative to Lutregala**	**This study**	**WA-PLS**	**Foraminifera**	**65**	**0.07**	**0.47**	**14.9**

Table 4 Comparisons of model performance and mean tidal range from multiple regions across the globe. Good model performance is recognised by a lower root mean squared error of performance (RMSEP). N – number of samples within training set. WA – Weighted Averaging regression, WA-Tol — Tolerance Down-Weighted Weighted Averaging regression, WAPLS — Weighted-Average Partial-Least-Squares regression, PLS — Partial-Least-Squares regression, ML – Maximum Likelihood. Table updated from those published by Barlow et al. (2013), Barnett et al. (2017), Callard et al. (2011) and Mills et al. (2013) combining and adding studies that utilise either diatoms, benthic foraminifera, testate amoebae, pollen or multiproxy (diatoms, foraminifera and testates combined) for sea-level reconstruction. We omit the Horton et al. (2007) subtidal transfer function from the analysis as this represents a large outlier in the dataset.
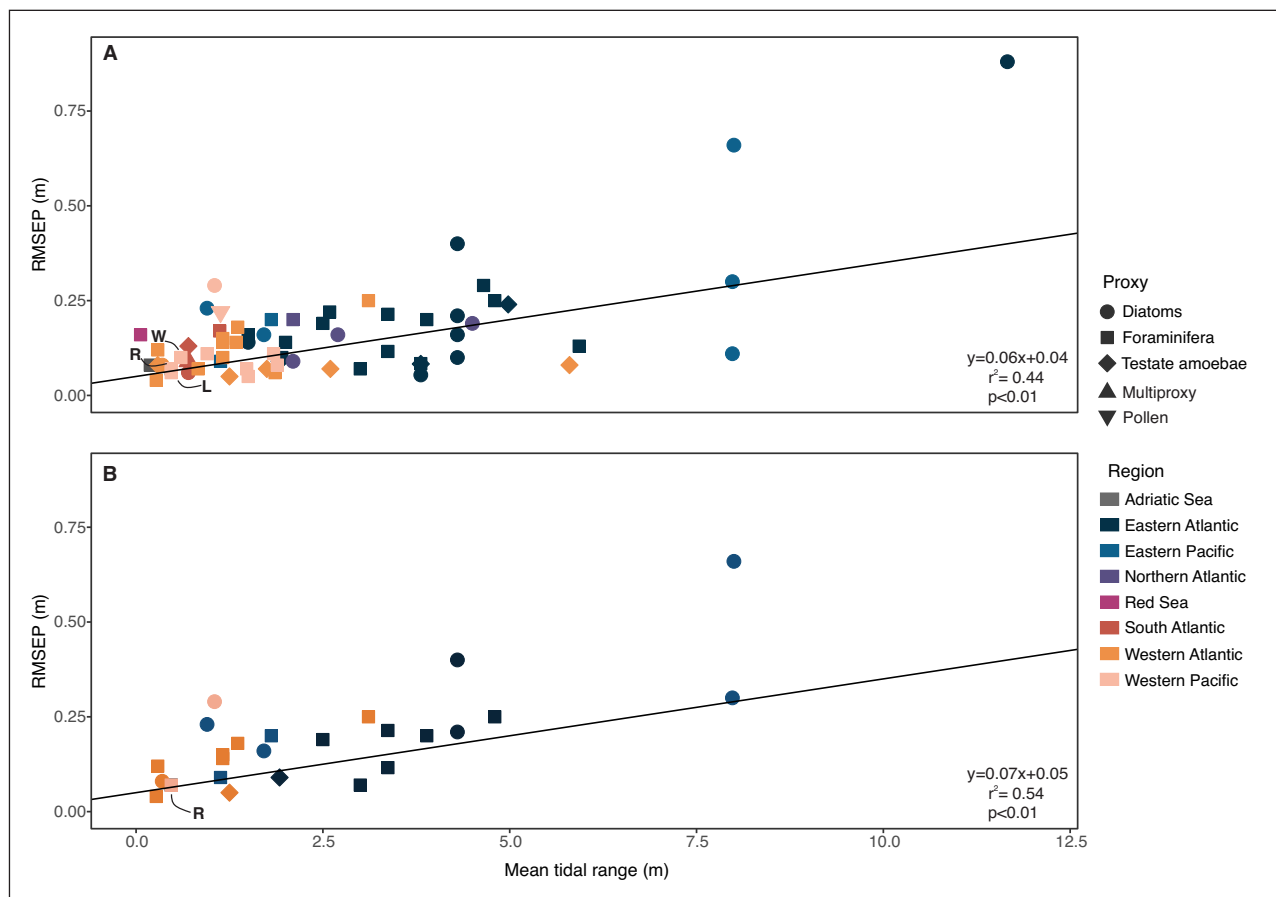
Figure 8 A. Relationship between model performance (root mean squared error of prediction; RMSEP) and mean tidal range (MTR) across 67 models (**Table 4**) including the Lutregala **(L)** and Wapengo **(W)** local training sets and the regional II model **(R)**. The updated dataset integrates training sets that use diatoms, benthic foraminifera, testate amoebae, pollen and multiproxy (diatoms, foraminifera and testates combined) approaches for sea-level reconstruction from multiple regions of the world. **B.** Relationship between model performance and mean tidal range showing only regional models.

reconstruction north and southwards of the previous site. Multivariate analyses identify three clusters within the combined regional foraminiferal training set, comprising a high elevation biozone, a mid-elevation biozone and a mid to low elevation biozone. Similar to contemporary foraminiferal distributions reported elsewhere in Australia and New Zealand, *T. inflata* is dominant at all sites and found along the majority of the sampled elevation gradient. No samples from Little Swanport are classified into the mid to low elevation cluster; we attribute this to the low and variable salinity in the Little Swanport estuary.

New local transfer functions for Lutregala and Wapengo perform well, with an ability to predict sea level within ± 0.06 m (68% confidence) or ± 0.12 m (95% confidence), and ± 0.11 m (68% confidence) or ± 0.22 m (95% confidence), respectively. The dominance of *T. inflata* and near-absence of *M. fusca* at Little Swanport complicates the development of a transfer function model that incorporates all three sites. Rather, a model combining the two higher salinity sites provides improved performance (RMSEP = 7.66 SWLI units) despite the large distance between these sites. When developing regional training sets, we advocate that the similarity in the

environmental settings (particularly salinity) should be assessed as an alternative way of grouping sites, rather than simply using spatial proximity.

Our transfer functions provide comparable predictive ability to other transfer functions reported elsewhere in Australia and New Zealand (*e.g.* Callard et al. 2011; Southall et al. 2006). By updating a global database of transfer function model performance we also show that our models are comparable with studies in distant regions, namely those from the western Atlantic. Our revised database of studies that use diatoms, benthic foraminifera, testate amoebae and pollen for sea-level reconstruction demonstrates that model performance is superior in locations with microtidal regimes. Future sea-level reconstructions from the microtidal coasts of New South Wales and Tasmania underpinned by the work presented here offer the potential for sea-level reconstructions with low vertical uncertainties that will help to refine understanding of late Holocene sea-level change in Australia as well as shed light on the discrepancy in rates of sea-level rise observed in proxy and instrumental records in the western Pacific, and help to elucidate the causes of the early 20th century sea-level acceleration.

ADDITIONAL FILES

Data availability (Supplementary file 1): Percentage counts of unscreened dead contemporary foraminifera as well as elevation data expressed in m AHD and tide-gauge data.
Code availability: Code used to compute the multivariate and transfer function analyses as well as to generate the figures within this publication are available through figshare: *https://doi.org/10.6084/m9.figshare.14573358* or see *https://figshare.com/authors/Sophie_Williams/9360050*. All assemblage figures in this publication were created in R package '*tidypalaeo*' (Dunnington, 2021).

TRAINING SET	DCA AXIS 1	DCA AXIS 2	DCA AXIS 3	DCA AXIS 4
Lutregala	0.56	0.24	0.12	0.13
Wapengo	0.72	0.26	0.30	0.17
Regional	0.65	0.33	0.22	0.22

Table S1 Detrended Correspondence Analysis axis scores for the Lutregala, Wapengo and Regional (Lutregala, Wapengo and Little Swanport combined) training sets.

- **Lay Summary.** New salt-marsh foraminifera training sets for late Holocene sea-level reconstruction in southeastern Australia. DOI: *https://doi.org/10.5334/oq.93.s1*

- **Supplementary information.** Foraminifera and elevation data associated with this publication. DOI: *https://doi.org/10.5334/oq.93.s2*

Figure S1 Transfer function performance for sub-regional **A.** and regional I training sets **B.** showing plateauing of Little Swanport samples when combined with the Lutregala and Wapengo training sets. Data are presented with elevation converted to Standardised Water-Level Index (SWLI). 95% prediction uncertainties are given for each sample.

Department who provided support during the field campaign as well as to Nick Bowden for establishing benchmarks at Lutregala and Little Swanport. Finally, we thank Maria Gehrels and Mike Beckwith at the University of York and technical staff at the School of Earth and Environmental Sciences, the University of Queensland for their support.

COMPETING INTERESTS

AUTHOR CONTRIBUTIONS

SW: Substantial contribution to fieldwork and writing of the manuscript, as well as conducting associated laboratory work, statistical analyses and creating figures for this paper. EG: Substantial contribution to the writing of the manuscript as well as conducting all tidal modelling. PM: Substantial contribution to fieldwork and writing of the manuscript. RB: Substantial contribution to fieldwork and vegetation data acquisition. RG: Substantial contribution to fieldwork, designer of the concept of the project and writing of the manuscript.

AUTHOR AFFILIATIONS

Sophie Williams *orcid.org/0000-0002-5122-9492*
University of York, GB

Ed Garrett *orcid.org/0000-0001-9985-0651*
University of York, GB

Patrick Moss *orcid.org/0000-0003-1546-9242*
University of Queensland, AU

Rebecca Bartlett
University of York, GB

Roland Gehrels *orcid.org/0000-0002-5088-5834*
University of York, GB

REFERENCES

Abu-Zied, RH and **Bantan, RA.** 2013. Hypersaline benthic foraminifera from the Shuaiba Lagoon, eastern Red Sea, Saudi Arabia: Their environmental controls and usefulness in sea-level reconstruction. *Marine Micropaleontology*, 103: 51–67. DOI: *https://doi.org/10.1016/j.marmicro.2013.07.005*

Apthorpe, M. 1980. Foraminiferal distribution in the estuarine Gippsland Lakes system, Victoria. *Proceedings of the Royal Society of Victoria*.

Australian Government, Department of Defence. 2020. *Australian National Tide Tables 2020*. Wollongong, New South Wales: Australian hydrographic office.

Avnaim-Katav, S, Gehrels, WR, Brown, LN, Fard, E and **MacDonald, GM.** 2017. Distributions of salt-marsh

foraminifera along the coast of SW California, USA: Implications for sea-level reconstructions. *Marine Micropaleontology*, 131: 25–43. DOI: *https://doi.org/10.1016/j.marmicro.2017.02.001*

Barlow, NLM, Shennan, I and **Long, AJ.** 2012. Relative sea-level response to Little Ice Age ice mass change in south central Alaska: Reconciling model predictions and geological evidence. *Earth and Planetary Science Letters*, 315–316: 62–75. DOI: *https://doi.org/10.1016/j.epsl.2011.09.048*

Barlow, NLM, Shennan, I, Long, AJ, Gehrels, WR, Saher, MH, Woodroffe, SA and **Hillier, C.** 2013. Salt marshes as late Holocene tide gauges. *Global and Planetary Change*, 106: 90–110. DOI: *https://doi.org/10.1016/j.gloplacha.2013.03.003*

Barnett, RL. 2013. Testate amoebae as sea-level indicators in northwestern Norway: developments in sample preparation and analysis. *Acta Protozoologica*, 52(3). DOI: *https://doi.org/10.4467/16890027AP.13.0012.1109*

Barnett, RL, Bernatchez, P, Garneau, M, Brain, MJ, Charman, DJ, Stephenson, DB, Haley, S and **Sanderson, N.** 2019. Late Holocene sea-level changes in eastern Québec and potential drivers. *Quaternary Science Reviews*, 203: 151–169. DOI: *https://doi.org/10.1016/j.quascirev.2018.10.039*

Barnett, RL, Garneau, M and **Bernatchez, P.** 2016. Salt-marsh sea-level indicators and transfer function development for the Magdalen Islands in the Gulf of St. Lawrence, Canada. *Marine Micropaleontology*, 122: 13–26. DOI: *https://doi.org/10.1016/j.marmicro.2015.11.003*

Barnett, RL, Gehrels, WR, Charman, DJ, Saher, MH and **Marshall, WA.** 2015. Late Holocene sea-level change in Arctic Norway. *Quaternary Science Reviews*, 107: 214–230. DOI: *https://doi.org/10.1016/j.quascirev.2014.10.027*

Barnett, RL, Newton, TL, Charman, DJ and **Gehrels, WR.** 2017. Salt-marsh testate amoebae as precise and widespread indicators of sea-level change. *Earth-Science Reviews*, 164: 193–207. DOI: *https://doi.org/10.1016/j.earscirev.2016.11.002*

Berkeley, A, Perry, CT, Smithers, SG and **Horton, BP.** 2008. The spatial and vertical distribution of living (stained) benthic foraminifera from a tropical, intertidal environment, north Queensland, Australia. *Marine Micropaleontology*, 69(2): 240–261. DOI: *https://doi.org/10.1016/j.marmicro.2008.08.002*

Berkeley, A, Perry, CT, Smithers, SG, Horton, BP and **Cundy, AB.** 2009. Foraminiferal biofacies across mangrove-mudflat environments at Cocoa Creek, north Queensland, Australia. *Marine Geology*, 263(1): 64–86. DOI: *https://doi.org/10.1016/j.margeo.2009.03.019*

Birks, HJB, Maddy, D and **Brew, JS.** 1995. Chapter 6: Quantitative Palaeoenvironmental Reconstructions. In: Brew, JS (ed.), *Statistical Modelling of Quaternary Science Data, Technical Guide*. 5. Cambridge: Quaternary Research Association. 161–254.

Bjørk, AA, Kjær, KH, Korsgaard, NJ, Khan, SA, Kjeldsen, KK, Andresen, CS, Box, JE, Larsen, NK and **Funder, S.** 2012. An aerial view of 80 years of climate-related glacier fluctuations in southeast Greenland. *Nature Geoscience*, 5(6): 427–432. DOI: *https://doi.org/10.1038/ngeo1481*

Brain, MJ, Long, AJ, Woodroffe, SA, Petley, DN, Milledge, DG and **Parnell, AC.** 2012. Modelling the effects of sediment compaction on salt marsh reconstructions of recent sea-level rise. *Earth and Planetary Science Letters*, 345–348: 180–193. DOI: *https://doi.org/10.1016/j.epsl.2012.06.045*

Bryant, SL. 2018. *Mammals on Lutregala Marsh Reserve, Bruny Island 2015–2017*. Tasmanian Land Conservancy, Lower Sandy Bay, Tasmania 7005. Available at: *https://tasland. org.au/content/uploads/2015/06/Mammals-on-Lutregala-Marsh-Reserve-2015-2017.pdf*.

Cahill, N, Kemp, AC, Horton, BP and **Parnell, AC.** 2016. A Bayesian hierarchical model for reconstructing relative sea level: from raw data to rates of change. *Climate of the Past*, 12(2): 525–542. DOI: *https://doi.org/10.5194/cp-12-525-2016*

Callard, SL, Gehrels, WR, Morrison, BV and **Grenfell, HR.** 2011. Suitability of salt-marsh foraminifera as proxy indicators of sea level in Tasmania. *Marine Micropaleontology*, 79 (3–4), Suitability of salt-marsh foraminifera as proxy indicators of sea level in Tasmania. *Marine Micropaleontology*, 79(3–4): 121–131. DOI: *https://doi.org/10.1016/j. marmicro.2011.03.001*

Camacho, SG, Moura, DM, Connor, S, Scott, DB and **Boski, T.** 2015. Taxonomy, ecology and biogeographical trends of dominant benthic foraminifera species from an Atlantic-Mediterranean estuary (the Guadiana, southeast Portugal). *Palaeontologia Electronica*, 18(1): 1–27. DOI: *https://doi. org/10.26879/512*

Cann, JH, Belperio, AP, Gostin, VA and **Rice, RL.** 1993. Contemporary benthic foraminifera in Gulf St Vincent, South Australia, and a refined Late Pleistocene sea-level history. *Australian Journal of Earth Sciences*, 40(2): 197–211. DOI: *https://doi.org/10.1080/08120099308728074*

Charman, DJ, Gehrels, WR, Manning, C and **Sharma, C.** 2010. Reconstruction of recent sea-level change using testate amoebae. *Quaternary Research*, 73(2): 208–219. DOI: *https://doi.org/10.1016/j.yqres.2009.11.009*

Chen, H, Shaw, TA, Wang, J, Engelhart, S, Nikitina, D, Pilarczyk, JE, Walker, J, García-Artola, A and **Horton, BP.** 2020. Salt-Marsh Foraminiferal Distributions from Mainland Northern Georgia, USA: An Assessment of Their Viability for Sea-Level Studies. *Open Quaternary*, 6(1): 1–19. DOI: *https://doi.org/10.5334/oq.80*

Clark, K, Cochran, U and **Mazengarb, C.** 2011. Holocene coastal evolution and evidence for paleotsunami from a tectonically stable region, Tasmania, Australia. *The Holocene*, 21(6): 883–895. DOI: *https://doi. org/10.1177/0959683610391317*

Crawford, C and **Mitchell, I.** 1999. *Physical and chemical parameters of several oyster growing areas in Tasmania*. Technical, Tasmanian Aquaculture & Fisheries Institute, Tasmania. Available at: *https://eprints.utas.edu.au/6653/1/ Tech_Report_4_PhysicalChemicall.pdf*.

Creese, RG, Glasby, TM, West, G and **Gallen, C.** 2009. *Mapping the habitats of NSW estuaries*. Industry & Investment NSW. Nelson Bay, New South Wales. 97. Available at: *http://www. friendsoftuggerahlakes-cen.org.au/SEAGRASS/2009%20 09%2000%20Industry%20and%20Investment%20Habitat-Mapping-Final-Report.pdf*.

de Rijk, S and **Troelstra, SR.** 1997. Salt marsh foraminifera from the Great Marshes, Massachusetts: environmental controls. *Palaeogeography, Palaeoclimatology, Palaeoecology*, 130(1): 81–112. DOI: *https://doi.org/10.1016/S0031-0182(96)00131-9*

Dean, LF and **De Deckker, P.** 2013. Recent benthic foraminifera from Twofold Bay, Eden NSW: community structure, biotopes and distribution controls. *Australian Journal of Earth Sciences*, 60(4): 475–496. DOI: *https://doi.org/10.1080 /08120099.2013.792294*

Dunnington, D. 2021. *Tidy Tools for Paleoenvironmental Archives [R package tidypaleo version 0.1.1]*. Comprehensive R Archive Network (CRAN). Available at: *https://CRAN.R-project.org/package=tidypaleo*.

Edwards, R and **Wright, A.** 2015. Chapter 13: Foraminifera. In: Shennan, I, Long, AJ and Horton, BP (eds.), *Handbook of Sea-Level Research*. Chichester, UK: John Wiley & Sons, Ltd. 191–217. DOI: *https://doi.org/10.1002/9781118452547. ch13*

Edwards, RJ and **Horton, BP.** 2000. Reconstructing relative sea-level change using UK salt-marsh foraminifera. *Marine Geology*, 169(1): 41–56. DOI: *https://doi.org/10.1016/ S0025-3227(00)00078-5*

Edwards, RJ, Wright, AJ and **van de Plassche, O.** 2004. Surface distributions of salt-marsh foraminifera from Connecticut, USA: modern analogues for high-resolution sea level studies. *Marine Micropaleontology*, 51(1): 1–21. DOI: *https:// doi.org/10.1016/j.marmicro.2003.08.002*

Egbert, GD and **Erofeeva, S.** 2010. OSU Tidal Data Inversion. *Oregon State University*.

Engelhart, SE, Horton, BP, Roberts, DH, Bryant, CL and **Corbett, DR.** 2007. Mangrove pollen of Indonesia and its suitability as a sea-level indicator. *Marine Geology*, 242(1): 65–81. DOI: *https://doi.org/10.1016/j.margeo.2007.02.020*

Farmer, N and **Forsyth, SM.** 1993. *Dover Sheet. Geological Atlas 1:50,000*. Tasmania Department of Mines.

Fatela, F and **Taborda, R.** 2002. Confidence limits of species proportions in microfossil assemblages. *Marine Micropaleontology*, 45(2): 169–174. DOI: *https://doi. org/10.1016/S0377-8398(02)00021-X*

Figueira, B and **Hayward, BW.** 2014. Impact of reworked foraminifera from an eroding salt marsh on sea-level studies, New Zealand. *New Zealand Journal of Geology and Geophysics*, 57(4): 378–389. DOI: *https://doi.org/10.1080/00 288306.2014.924971*

FitzGerald, DM and **Hughes, Z.** 2019. Marsh Processes and Their Response to Climate Change and Sea-Level Rise. *Annual Review of Earth and Planetary Sciences*, 47(1): 481–517. DOI: *https://doi.org/10.1146/annurev-earth-082517-010255*

Fleming, KM, Tregoning, P, Kuhn, M, Purcell, A and **McQueen, H.** 2012. The effect of melting land-based ice masses on sea-level around the Australian coastline. *Australian Journal*

of Earth Sciences, 59(4): 457–467. DOI: *https://doi.org/10.10 80/08120099.2012.664828*

Frederikse, T, Adhikari, S, Daley, TJ, Dangendorf, S, Gehrels, WR, Landerer, F, Marcos, M, Newton, TL, Rush, G, Slangen, ABA and **Wöppelmann, G.** 2021. Constraining 20th-Century Sea-Level Rise in the South Atlantic Ocean. *Journal of Geophysical Research: Oceans*, 126(3): p.e2020JC016970. DOI: *https://doi.org/10.1029/2020JC016970*

Garside, CJ, Glasby, TM, Coleman, MA, Kelaher, BP and **Bishop, MJ.** 2014. The frequency of connection of coastal water bodies to the ocean predicts *Carcinus maenas* invasion. *Limnology and Oceanography*, 59(4): 1288–1296. DOI: *https://doi.org/10.4319/lo.2014.59.4.1288*

Gehrels, WR. 2000. Using foraminiferal transfer functions to produce high-resolution sea-level records from salt-marsh deposits, Maine, USA. *The Holocene*, 10(3): 367–376. DOI: *https://doi.org/10.1191/095968300670746884*

Gehrels, WR, Callard, SL, Moss, PT, Marshall, WA, Blaauw, M, Hunter, J, Milton, JA and **Garnett, MH.** 2012. Nineteenth and twentieth century sea-level changes in Tasmania and New Zealand. *Earth and Planetary Science Letters*, 315–316: 94–102. DOI: *https://doi.org/10.1016/j.epsl.2011.08.046*

Gehrels, WR, Dangendorf, S, Barlow, NLM, Saher, MH, Long, AJ, Woodworth, PL, Piecuch, CG and **Berk, K.** 2020. A Preindustrial Sea-Level Rise Hotspot Along the Atlantic Coast of North America. *Geophysical Research Letters*, 47(4): p.e2019GL085814. DOI: *https://doi. org/10.1029/2019GL085814*

Gehrels, WR, Hayward, BW, Newnham, RM and **Southall, KE.** 2008. A 20th century acceleration of sea-level rise in New Zealand. *Geophysical Research Letters*, 35(2): p.L02717. DOI: *https://doi.org/10.1029/2007GL032632*

Gehrels, WR, Hendon, D and **Charman, DJ.** 2006. Distribution of testate amoebae in salt marshes along the North American East Coast. *Journal of Foraminiferal Research*, 36(3): 201–214. DOI: *https://doi.org/10.2113/gsjfr.36.3.201*

Gehrels, WR, Kirby, JR, Prokoph, A, Newnham, RM, Achterberg, EP, Evans, H, Black, S and **Scott, DB.** 2005. Onset of recent rapid sea-level rise in the western Atlantic Ocean. *Quaternary Science Reviews*, 24(18–19): 2083–2100. DOI: *https://doi.org/10.1016/j.quascirev.2004.11.016*

Gehrels, WR, Marshall, WA, Gehrels, MJ, Larsen, GN, Kirby, JR, Eiríksson, JN, Heinemeier, J and **Shimmield, T.** 2006. Rapid sea-level rise in the North Atlantic Ocean since the first half of the nineteenth century. *The Holocene*, 16(7): 949–965. DOI: *https://doi.org/10.1177/0959683606hl986rp*

Gehrels, WR and **Newman, SWG.** 2004. Salt-marsh foraminifera in Ho Bugt, western Denmark, and their use as sea-level indicators. *Geografisk Tidsskrift-Danish Journal of Geography*, 104(1): 97–106. DOI: *https://doi.org/10.1080/00 167223.2004.10649507*

Gehrels, WR, Roe, HM and **Charman, DJ.** 2001. Foraminifera, testate amoebae and diatoms as sea-level indicators in UK saltmarshes: a quantitative multiproxy approach. *Journal of Quaternary Science*, 16(3): 201–220. DOI: *https://doi. org/10.1002/jqs.588*

Gerlach, MJ, Engelhart, SE, Kemp, AC, Moyer, RP, Smoak, JM, Bernhardt, CE and **Cahill, N.** 2017. Reconstructing Common Era relative sea-level change on the Gulf Coast of Florida. *Marine Geology*, 390: 254–269. DOI: *https://doi. org/10.1016/j.margeo.2017.07.001*

Gomez, N, Mitrovica, JX, Tamisiea, ME and **Clark, PU.** 2010. A new projection of sea level change in response to collapse of marine sectors of the Antarctic Ice Sheet. *Geophysical Journal International*, 180(2): 623–634. DOI: *https://doi. org/10.1111/j.1365-246X.2009.04419.x*

Grenfell, HR, Hayward, BW, Nomura, R and **Sabaa, AT.** 2012. A foraminiferal proxy record of 20th century sea-level rise in the Manukau Harbour, New Zealand. *Marine and Freshwater Research*, 63(4): 370–384. DOI: *https://doi.org/10.1071/ MF11208*

Hamilton, S and **Shennan, I.** 2005. Late Holocene relative sea-level changes and the earthquake deformation cycle around upper Cook Inlet, Alaska. *Quaternary Science Reviews*, 24(12): 1479–1498. DOI: *https://doi.org/10.1016/j. quascirev.2004.11.003*

Haslett, SK. 2001. The Palaeoenvironmental Implications of the Distribution of Intertidal Foraminifera in a Tropical Australian Estuary: a Reconnaissance Study. *Australian Geographical Studies*, 39(1): 67–74. DOI: *https://doi. org/10.1111/1467-8470.00130*

Haslett, SK, Davies-Burrows, R, Panayotou, K, Jones, BG and **Woodroff, CD.** 2010. Holocene evolution of the Minnamurra River estuary, southeast Australia: foraminiferal evidence. *Zeitschrift für Geomorphologie, Supplementary Issues*, 54(3): 79–98. DOI: *https://doi.org/10.1127/0372- 8854/2010/0054S3-0020*

Hawkes, AD, Horton, BP, Nelson, AR and **Hill, DF.** 2010. The application of intertidal foraminifera to reconstruct coastal subsidence during the giant Cascadia earthquake of AD 1700 in Oregon, USA. *Quaternary International*, 221(1–2): 116–140. DOI: *https://doi.org/10.1016/j. quaint.2009.09.019*

Hayward, BW. 2014. 'Monospecific' and near-monospecific benthic foraminiferal faunas, New Zealand. *The Journal of Foraminiferal Research*, 44(3): 300–315. DOI: *https://doi. org/10.2113/gsjfr.44.3.300*

Hayward, BW, Grenfell, HR and **Scott, DB.** 1999. Tidal range of marsh foraminifera for determining former sealevel heights in New Zealand. *New Zealand Journal of Geology and Geophysics*, 42(3): 395–413. DOI: *https://doi.org/10.1080/00 288306.1999.9514853*

Hayward, BW and **Hollis, CJ.** 1994. Brackish Foraminifera in New Zealand: A Taxonomic and Ecologic Review. *Micropaleontology*, 40(3): 185–222. DOI: *https://doi. org/10.2307/1485816*

Hayward, BW, Le Coze, F and **Gross, O.** 2019. *Catalogue of Life: WoRMS Foraminifera*. Available at: *https://www. catalogueoflife.org/col/details/database/id/157* [Accessed 14 October 2020].

Hedge, P and **Kriwoken, LK.** 2000. Evidence for effects of *Spartina anglica* invasion on benthic macrofauna in

Little Swanport estuary, Tasmania. *Austral Ecology*, 25(2): 150–159. DOI: *https://doi.org/10.1046/j.1442-9993.2000.01016.x*

Hegerl, GC, Brönnimann, S, Schurer, A and **Cowan, T.** 2018. The early 20th century warming: Anomalies, causes, and consequences. *Wiley Interdisciplinary Reviews: Climate Change*, 9(4): p.e522. DOI: *https://doi.org/10.1002/wcc.522*

Hill, MO and **Gauch, HG.** 1980. Detrended correspondence analysis: an improved ordination technique. In: van der Maarel, E (ed.), *Classification and ordination*. Dordrecht, Netherlands: Springer. 47–58. DOI: *https://doi.org/10.1007/978-94-009-9197-2_7*

Hill, TC, Woodland, WA, Spencer, CD and **Marriott, SB.** 2007. Holocene sea-level change in the Severn Estuary, southwest England: a diatom-based sea-level transfer function for macrotidal settings. *The Holocene*, 17(5): 639–648. DOI: *https://doi.org/10.1177/0959683607078988*

Hocking, EP, Garrett, E and **Cisternas, M.** 2017. Modern diatom assemblages from Chilean tidal marshes and their application for quantifying deformation during past great earthquakes. *Journal of Quaternary Science*, 32(3): 396–415. DOI: *https://doi.org/10.1002/jqs.2933*

Holgate, SJ, Matthews, A, Woodworth, PL, Rickards, LJ, Tamisiea, ME, Bradshaw, E, Foden, PR, Gordon, KM, Jevrejeva, S and **Pugh, J.** 2013. New Data Systems and Products at the Permanent Service for Mean Sea Level. *Journal of Coastal Research*, 29(3): 493–504. DOI: *https://doi.org/10.2112/JCOASTRES-D-12-00175.1*

Horton, BP, Corbett, R, Culver, SJ, Edwards, RJ and **Hillier, C.** 2006. Modern saltmarsh diatom distributions of the Outer Banks, North Carolina, and the development of a transfer function for high resolution reconstructions of sea level. *Estuarine, Coastal and Shelf Science*, 69(3): 381–394. DOI: *https://doi.org/10.1016/j.ecss.2006.05.007*

Horton, BP, Culver, SJ, Hardbattle, MIJ, Larcombe, P, Milne, GA, Morigi, C, Whittaker, JE and **Woodroffe, SA.** 2007. Reconstructing Holocene sea-level change for the central Great Barrier Reef (Australia) using subtidal foraminifera. *Journal of Foraminiferal Research*, 37(4): 327–343. DOI: *https://doi.org/10.2113/gsjfr.37.4.327*

Horton, BP and **Edwards, RJ.** 2005. The application of local and regional transfer functions to the reconstruction of Holocene sea levels, north Norfolk, England. *The Holocene*, 15(2): 216–228. DOI: *https://doi.org/10.1191/0959683605hl787rp*

Horton, BP and **Edwards, RJ.** 2006. *Quantifying Holocene Sea Level Change Using Intertidal Foraminifera: Lessons from the British Isles.* Available at: *https://repository.upenn.edu/cgi/viewcontent.cgi?article=1050&context=ees_papers.*

Horton, BP, Edwards, RJ and **Lloyd, JM.** 1999. A foraminiferal-based transfer function: implications for sea-level studies. *Journal of Foraminiferal Research*, 29(2): 117–129. DOI: *https://doi.org/10.2113/gsjfr.29.2.117*

Horton, BP, Larcombe, P, Woodroffe, SA, Whittaker, JE, Wright, MR and **Wynn, C.** 2003. Contemporary foraminiferal distributions of a mangrove environment, Great Barrier Reef coastline, Australia: implications for sea-level reconstructions. *Marine Geology*, 198(3): 225–243. DOI: *https://doi.org/10.1016/S0025-3227(03)00117-8*

Horton, BP and **Murray, JW.** 2006. Patterns in cumulative increase in live and dead species from foraminiferal time series of Cowpen Marsh, Tees Estuary, UK: Implications for sea-level studies. *Marine Micropaleontology*, 58(4): 287–315. DOI: *https://doi.org/10.1016/j.marmicro.2005.10.006*

Horton, BP and **Murray, JW.** 2007. The roles of elevation and salinity as primary controls on living foraminiferal distributions: Cowpen Marsh, Tees Estuary, UK. *Marine Micropaleontology*, 63(3): 169–186. DOI: *https://doi.org/10.1016/j.marmicro.2006.11.006*

Juggins, S. 2013. Quantitative reconstructions in palaeolimnology: new paradigm or sick science? *Quaternary Science Reviews*, 64: 20–32. DOI: *https://doi.org/10.1016/j.quascirev.2012.12.014*

Juggins, S. 2020. *Package 'rioja'.* Available at: *https://cran.r-project.org/web/packages/rioja/rioja.pdf.*

Juggins, S and **Birks, HJB.** 2012. Quantitative Environmental Reconstructions from Biological Data. In: Birks, HJB, Lotter, AF, Juggins, S and Smol, JP (eds.), *Tracking Environmental Change Using Lake Sediments: Data Handling and Numerical Techniques*. Developments in Paleoenvironmental Research. Dordrecht, Netherlands: Springer. 431–494. DOI: *https://doi.org/10.1007/978-94-007-2745-8_14*

Kassambara, A and **Mundt, F.** 2017. *Package 'factoextra'. Extract and visualize the results of multivariate data analyses.* Available at: *https://cran.microsoft.com/snapshot/2016-11-30/web/packages/factoextra/factoextra.pdf.*

Kaufman, L and **Rousseeuw, PJ.** 1990. *Finding Groups in Data: An Introduction to Cluster Analysis.* 344. New York: John Wiley & Sons. DOI: *https://doi.org/10.1002/9780470316801*

Kelleway, JJ, Saintilan, N, Macreadie, PI, Baldock, JA, Heijnis, H, Zawadzki, A, Gadd, P, Jacobsen, G and **Ralph, PJ.** 2017. Geochemical analyses reveal the importance of environmental history for blue carbon sequestration. *Journal of Geophysical Research: Biogeosciences*, 122(7): 1789–1805. DOI: *https://doi.org/10.1002/2017JG003775*

Kemp, AC, Hill, TD, Vane, CH, Cahill, N, Orton, PM, Talke, SA, Parnell, AC, Sanborn, K and **Hartig, EK.** 2017a. Relative sea-level trends in New York City during the past 1500 years. *The Holocene*, 27(8): 1169–1186. DOI: *https://doi.org/10.1177/0959683616683263*

Kemp, AC, Horton, BP and **Culver, SJ.** 2009. Distribution of modern salt-marsh foraminifera in the Albemarle–Pamlico estuarine system of North Carolina, USA: Implications for sea-level research. *Marine Micropaleontology*, 72(3–4): 222–238. DOI: *https://doi.org/10.1016/j.marmicro.2009.06.002*

Kemp, AC, Horton, BP, Culver, SJ, Corbett, DR, van de Plassche, O, Gehrels, WR, Douglas, BC and **Parnell, AC.** 2009. Timing and magnitude of recent accelerated sea-level rise (North Carolina, United States). *Geology*, 27(11): 1035–1038. DOI: *https://doi.org/10.1130/G30352A.1*

Kemp, AC, Horton, BP, Nikitina, D, Vane, CH, Potapova, M, Weber-Bruya, E, Culver, SJ, Repkina, T and **Hill, DF.** 2017b. The distribution and utility of sea-level indicators in Eurasian sub-Arctic salt marshes (White Sea, Russia). *Boreas*, 46(3): 562–584. DOI: *https://doi.org/10.1111/bor.12233*

Kemp, AC, Horton, BP, Vann, DR, Engelhart, SE, Pre, CAG, Vane, CH, Nikitina, D and **Anisfeld, SC.** 2012. Quantitative vertical zonation of salt-marsh foraminifera for reconstructing former sea level; an example from New Jersey, USA. *Quaternary Science Reviews*, 54: 26–39. DOI: *https://doi.org/10.1016/j.quascirev.2011.09.014*

Kemp, AC and **Telford, RJ.** 2015. Chapter 31: Transfer functions. In: Shennan, I, Long, AJ and Horton BP (eds). *Handbook of Sea-Level Research*. John Wiley & Sons. *Handbook of Sea-Level Research*. Chichester, UK: John Wiley & Sons, Ltd. 470–499. DOI: *https://doi.org/10.1002/9781118452547.ch31*

Kemp, AC, Telford, RJ, Horton, BP, Anisfeld, SC and **Sommerfield, CK.** 2013. Reconstructing Holocene sea level using salt-marsh foraminifera and transfer functions: lessons from New Jersey, USA. *Journal of Quaternary Science*, 28(6): 617–629. DOI: *https://doi.org/10.1002/jqs.2657*

Kemp, AC, Wright, AJ and **Cahill, N.** 2020. Enough is Enough, or More is More? Testing the Influence of Foraminiferal Count Size on Reconstructions of Paleo-Marsh Elevation. *Journal of Foraminiferal Research*, 50(3): 266–278. DOI: *https://doi.org/10.2113/gsjfr.50.3.266*

Kemp, AC, Wright, AJ, Edwards, RJ, Barnett, RL, Brain, MJ, Kopp, RE, Cahill, N, Horton, BP, Charman, DJ, Hawkes, AD and **Hill, TD.** 2018. Relative sea-level change in Newfoundland, Canada during the past 3000 years. *Quaternary Science Reviews*, 201: 89–110. DOI: *https://doi.org/10.1016/j.quascirev.2018.10.012*

Kjeldsen, KK, Korsgaard, NJ, Bjørk, AA, Khan, SA, Box, JE, Funder, S, Larsen, NK, Bamber, JL, Colgan, W, van den Broeke, M and **Siggaard-Andersen, ML.** 2015. Spatial and temporal distribution of mass loss from the Greenland Ice Sheet since AD 1900. *Nature*, 528(7582): 396–400. DOI: *https://doi.org/10.1038/nature16183*

Kopp, RE, Horton, BP, Kemp, AC and **Tebaldi, C.** 2015. Past and future sea-level rise along the coast of North Carolina, USA. *Climatic Change*, 132(4): 693–707. DOI: *https://doi.org/10.1007/s10584-015-1451-x*

Kopp, RE, Kemp, AC, Bittermann, K, Horton, BP, Donnelly, JP, Gehrels, WR, Hay, CC, Mitrovica, JX, Morrow, ED and **Rahmstorf, S.** 2016. Temperature-driven global sea-level variability in the Common Era. *Proceedings of the National Academy of Sciences of the United States of America*, 113(11): E1434–41. DOI: *https://doi.org/10.1073/pnas.1517056113*

Lal, KK, Bonetti, C, Woodroffe, CD and **Rogers, K.** 2020. Contemporary distribution of benthic foraminiferal assemblages in coastal wetlands of south-eastern Australia. *Estuarine, Coastal and Shelf Science*, 245: 106949. DOI: *https://doi.org/10.1016/j.ecss.2020.106949*

Leorri, E, Fatela, F, Cearreta, A, Moreno, J, Antunes, C and **Drago, T.** 2011. Assessing the performance of a foraminifera-based transfer function to estimate sea-level changes in northern Portugal. *Quaternary Research*, 75(1): 278–287. DOI: *https://doi.org/10.1016/j.yqres.2010.10.003*

Leorri, E, Gehrels, WR, Horton, BP, Fatela, F and **Cearreta, A.** 2010. Distribution of foraminifera in salt marshes along the Atlantic coast of SW Europe: Tools to reconstruct past sea-level variations. *Quaternary International*, 221(1): 104–115. DOI: *https://doi.org/10.1016/j.quaint.2009.10.033*

Leorri, E, Horton, BP and **Cearreta, A.** 2008. Development of a foraminifera-based transfer function in the Basque marshes, N. Spain: implications for sea-level studies in the Bay of Biscay. *Marine Geology*, 251(1–2): 60–74. DOI: *https://doi.org/10.1016/j.margeo.2008.02.005*

Long, AJ, Woodroffe, SA, Milne, GA, Bryant, CL and **Wake, LM.** 2010. Relative sea level change in west Greenland during the last millennium. *Quaternary Science Reviews*, 29(3): 367–383. DOI: *https://doi.org/10.1016/j.quascirev.2009.09.010*

Maechler, M, Rousseeuw, P, Struyf, A, Hubert, M, Hornik, K and **Studer, M.** 2013. *Package 'cluster'*. Available at: *https://cran.r-project.org/web/packages/cluster/cluster.pdf.*

Massey, AC, Gehrels, WR, Charman, DJ and **White, SV.** 2006. An intertidal foraminifera-based transfer function for reconstructing Holocene sea-level change in southwest England. *The Journal of Foraminiferal Research*, 36(3): 215–232. DOI: *https://doi.org/10.2113/gsjfr.36.3.215*

Milker, Y, Horton, BP, Nelson, AR, Engelhart, SE and **Witter, RC.** 2015a. Variability of intertidal foraminiferal assemblages in a salt marsh, Oregon, USA. *Marine Micropaleontology*, 118: 1–16. DOI: *https://doi.org/10.1016/j.marmicro.2015.04.004*

Milker, Y, Horton, BP, Vane, CH, Engelhart, SE, Nelson, AR, Witter, RC, Khan, NS and **Bridgeland, WT.** 2015b. Annual and seasonal distribution of intertidal foraminifera and stable carbon isotope geochemistry, Bandon Marsh, Oregon, USA. *The Journal of Foraminiferal Research*, 45(2): 146–155. DOI: *https://doi.org/10.2113/gsjfr.45.2.146*

Milker, Y, Nelson, AR, Horton, BP, Engelhart, SE, Bradley, LA and **Witter, RC.** 2016. Differences in coastal subsidence in southern Oregon (USA) during at least six prehistoric megathrust earthquakes. *Quaternary Science Reviews*, 142: 143–163. DOI: *https://doi.org/10.1016/j.quascirev.2016.04.017*

Mills, H, Kirby, J, Holgate, S and **Plater, A.** 2013. The distribution of contemporary saltmarsh foraminifera in a macrotidal estuary: an assessment of their viability for sea-level studies. *Journal of Ecosystem and Ecography*, 3: 1–16. DOI: *https://doi.org/10.4172/2157-7625.1000131*

Moss, PT, Gehrels, WR and **Callard, SL.** 2016. European Impacts on Coastal Eastern Tasmania: Insight from a High-

Resolution Palynological Analysis of a Salt-Marsh Core. *Frontiers in Ecology and Evolution*, 4: 105. DOI: *https://doi.org/10.3389/fevo.2016.00105*

Murray, JW. 2006. *Ecology and Applications of Benthic Foraminifera*. Cambridge University Press. DOI: *https://doi.org/10.1017/CBO9780511535529*

Murray, JW and **Bowser, SS.** 2000. Mortality, protoplasm decay rate, and reliability of staining techniques to recognize 'living' foraminifera: a review. *Journal of Foraminiferal Research*, 30(1): 66–70. DOI: *https://doi.org/10.2113/0300066*

Newton, TL, Gehrels, WR, Fyfe, RM and **Daley, TJ.** 2021. Reconstructing sea-level change in the Falkland Islands (Islas Malvinas) using salt-marsh foraminifera, diatoms and testate amoebae. *Marine Micropaleontology*, 162: 101923. DOI: *https://doi.org/10.1016/j.marmicro.2020.101923*

Oksanen, J, Kindt, R, Legendre, P, O'Hara, B, Stevens, MHH, Oksanen, MJ and **Suggests, MASS.** 2007. *The vegan package. Community ecology package*. Available at: *https://cran.ism.ac.jp/web/packages/vegan/vegan.pdf*

Ooms, M, Beyens, L and **Temmerman, S.** 2012. Testate amoebae as proxy for water level changes in a brackish tidal marsh. *Acta Protozoologica*, 51(3). DOI: *https://doi.org/10.4467/16890027AP.12.022.0768*

Ostrognay, DB and **Haig, DW.** 2012. Foraminifera from microtidal rivers with large seasonal salinity variation, southwest Western Australia. *Journal of the Royal Society of Western Australia*, 95: 137.

Parkes, D and **Marzeion, B.** 2018. Twentieth-century contribution to sea-level rise from uncharted glaciers. *Nature*, 563(7732): 551–554. DOI: *https://doi.org/10.1038/s41586-018-0687-9*

Parsons, K. 2012. *State of the D'Entrecasteaux Channel and the lower Huon Estuary 2012*. Kingston, Tasmania: Kingborough Council. Available at: *https://www.bien.org.au/wp-content/uploads/2019/09/State-of-Channel-lower-Huon_electronic-version_web.pdf*.

Pearce, I, Handlinger, JH and **Hallegraeff, GM.** 2005. Histopathology in Pacific oyster (*Crassostrea gigas*) spat caused by the dinoflagellate *Prorocentrum rhathymum*. *Harmful Algae*, 4(1): 61–74. DOI: *https://doi.org/10.1016/j.hal.2003.11.002*

Prahalad, V and **Jones, J.** 2013. *Mapping coastal saltmarshes in Southern Tasmania*. Tasmania: NRM South. Available at: *https://www.nrmsouth.org.au/wp-content/uploads/2014/10/Mapping-Coastal-Saltmarshes-in-Southern-Tasmania.pdf*.

R Core Team. 2020. *R: A language and environment for statistical computing.* Vienna, Austria: R Foundation for Statistical Computing. Available at: *https://www.R-project.org/*.

Rickard, MJ and **Love, S.** 2000. Timing of megakinks and related structures: Constraints from the Devonian Bunga-Wapengo Basin, Mimosa Rocks National Park, New South Wales. *Australian Journal of Earth Sciences*, 47(6): 1009–1013. DOI: *https://doi.org/10.1046/j.1440-0952.2000.00827.x*

Roper, T, Creese, B, Scanes, P, Stephens, K, Williams, R, Dela-Cruz, J, Coade, G, Coates, B and **Fraser, M.** 2011. Assessing the condition of estuaries and coastal lake ecosystems in NSW. *Monitoring, evaluation and reporting program*. Sydney: NSW Office of Environment and Heritage. Available at: *https://www.environment.nsw.gov.au/-/media/OEH/Corporate-Site/Documents/Water/State-of-the-catchments-2010/Technical-report-series/assessing-condition-estuaries-coastal-lake-ecosystems-110717.pdf.*

Rossi, V, Horton, BP, Corbett, DR, Leorri, E, Perez-Belmonte, L and **Douglas, BC.** 2011. The application of foraminifera to reconstruct the rate of 20th century sea level rise, Morbihan Golfe, Brittany, France. *Quaternary Research*, 75(1): 24–35. DOI: *https://doi.org/10.1016/j.yqres.2010.07.017*

Sachs, HM, Webb, T and **Clark, DR.** 1977. Paleoecological Transfer Functions. *Annual Review of Earth and Planetary Sciences*, 5(1): 159–178. DOI: *https://doi.org/10.1146/annurev.ea.05.050177.001111*

Saher, MH, Gehrels, WR, Barlow, NLM, Long, AJ, Haigh, ID and **Blaauw, M.** 2015. Sea-level changes in Iceland and the influence of the North Atlantic Oscillation during the last half millennium. *Quaternary Science Reviews*, 108: 23–36. DOI: *https://doi.org/10.1016/j.quascirev.2014.11.005*

Sakabe, R and **Lyle, JM.** 2010. The influence of tidal cycles and freshwater inflow on the distribution and movement of an estuarine resident fish *Acanthopagrus butcheri*. *Journal of Fish Biology*, 77(3): 643–660. DOI: *https://doi.org/10.1111/j.1095-8649.2010.02703.x*

Sawai, Y, Horton, BP and **Nagumo, T.** 2004. The development of a diatom-based transfer function along the Pacific coast of eastern Hokkaido, northern Japan—an aid in paleoseismic studies of the Kuril subduction zone. *Quaternary Science Reviews*, 23(23): 2467–2483. DOI: *https://doi.org/10.1016/j.quascirev.2004.05.006*

Scammell, MS, Batley, GE and **Brockbank, CI.** 1991. A field study of the impact on oysters of tributyltin introduction and removal in a pristine lake. *Archives of Environmental Contamination and Toxicology*, 20(2): 276–281. DOI: *https://doi.org/10.1007/BF01055916*

Scanes, P, Coade, G, Doherty, M and **Hill, R.** 2007. Evaluation of the utility of water quality based indicators of estuarine lagoon condition in NSW, Australia. *Estuarine, Coastal and Shelf Science*, 74(1–2): 306–319. DOI: *https://doi.org/10.1016/j.ecss.2007.04.021*

Schröder-Adams, CJ, Boyd, RL and **Tran, T.** 2014. Estuarine foraminiferal biofacies pattern compared to the brackish ichnofacies model: Port Stephens, southeast Australia. *Estuarine, Coastal and Shelf Science*, 139: 78–87. DOI: *https://doi.org/10.1016/j.ecss.2013.12.006*

Scott, DB and **Hermelin, JOR.** 1993. A device for precision splitting of micropaleontological samples in liquid suspension. *Journal of Paleontology*, 67(1): 151–154. DOI: *https://doi.org/10.1017/S0022336000021302*

Scott, DS and **Medioli, FS.** 1978. Vertical zonations of marsh foraminifera as accurate indicators of former sea-levels.

Nature, 272(5653): 528–531. DOI: *https://doi.org/10.1038/272528a0*

Shaw, TA, Kirby, JR, Holgate, S, Tutman, P and **Plater, AJ.** 2016. Contemporary salt-marsh foraminiferal distribution from the Adriatic coast of Croatia and its potential for sea-level studies. *The Journal of Foraminiferal Research*, 46(3): 314–332. DOI: *https://doi.org/10.2113/gsjfr.46.3.314*

Southall, KE, Gehrels, WR and **Hayward, BW.** 2006. Foraminifera in a New Zealand salt marsh and their suitability as sea-level indicators. *Marine Micropaleontology*, 60(2): 167–179. DOI: *https://doi.org/10.1016/j.marmicro.2006.04.005*

Stéphan, P, Goslin, J, Pailler, Y, Manceau, R, Suanez, S, Van Vliet-Lanoë, B, Hénaff, A and **Delacourt, C.** 2014. Holocene salt-marsh sedimentary infilling and relative sea-level changes in West Brittany (France) using foraminifera-based transfer functions. *Boreas*, 44(1): 153–177. DOI: *https://doi.org/10.1111/bor.12092*

Strachan, KL, Finch, JM, Hill, T and **Barnett, RL.** 2014. A late Holocene sea-level curve for the east coast of South Africa. *South African Journal of Science*, 110(1–2): 1–9. DOI: *https://doi.org/10.1590/sajs.2014/20130198*

Strachan, KL, Hill, TR, Finch, JM and **Barnett, RL.** 2015. Vertical zonation of foraminifera assemblages in Galpins salt marsh, South Africa. *Journal of Foraminiferal Research*, 45(1): 29–41. DOI: *https://doi.org/10.2113/gsjfr.45.1.29*

Strotz, LC. 2015. Spatial patterns and diversity of foraminifera from an intermittently closed and open lagoon, Smiths Lake, Australia. *Estuarine, Coastal and Shelf Science*, 164: 340–352. DOI: *https://doi.org/10.1016/j.ecss.2015.07.048*

Szkornik, K, Gehrels, WR and **Kirby, JR.** 2006. Salt-marsh diatom distributions in Ho Bugt (western Denmark) and the development of a transfer function for reconstructing Holocene sea-level changes. *Marine Geology*, 235(1–4): 137–150. DOI: *https://doi.org/10.1016/j.margeo.2006.10.010*

Telford, RJ. 2011. palaeoSig: significance tests of quantitative palaeoenvironmental reconstructions. *R package version*, 1. Available at: *https://cran.r-project.org/web/packages/palaeoSig/palaeoSig.pdf.*

ter Braak, CJ and **Juggins, S.** 1993. Weighted averaging partial least squares regression (WA-PLS): an improved method for reconstructing environmental variables from species assemblages. In: van Dam, H (ed.), *Twelfth international diatom symposium, Developments in Hydrobiology*, vol 90. Dordrecht, Netherlands: Springer. DOI: *https://doi.org/10.1007/978-94-017-3622-0_49*

ter Braak, CJF, Juggins, S, Birks, HJB and **van der Voet, H.** 1993. Chapter 25: Weighted averaging partial least squares regression (WA-PLS): definition and comparison with other methods for species-environment calibration. In: Patil, GP and Rao, CR (eds.), *Multivariate Environmental Statistics*. Amsterdam: Elsevier Science Publishers B.V. (North Holland), 525–560. DOI: *https://doi.org/10.1007/978-94-017-3622-0_49*

ter Braak, CJ and **Smilauer, P.** 2002. *CANOCO reference manual and CanoDraw for Windows user's guide: software for canonical community ordination (version 4.5)*. Available at: *www.canoco.com.*

ter Braak, CJF and **Verdonschot, PEM.** 1995. Canonical correspondence analysis and related multivariate methods in aquatic ecology. *Aquatic sciences*, 57(3): 255–289. DOI: *https://doi.org/10.1007/BF00877430*

Vermassen, F, Bjørk, AA, Sicre, MA, Jaeger, JM, Wangner, DJ, Kjeldsen, KK, Siggaard-Andersen, ML, Klein, V, Mouginot, J, Kjær, KH and **Andresen, CS.** 2020. A Major Collapse of Kangerlussuaq Glacier's Ice Tongue Between 1932 and 1933 in East Greenland. *Geophysical Research Letters*, 47(4): p.e2019GL085954. DOI: *https://doi.org/10.1029/2019GL085954*

Walker, JS, Cahill, N, Khan, NS, Shaw, TA, Barber, D, Miller, KG, Kopp, RE and **Horton, BP.** 2020. Incorporating temporal and spatial variability of salt-marsh foraminifera into sea-level reconstructions. *Marine Geology*, 429: 106293. DOI: *https://doi.org/10.1016/j.margeo.2020.106293*

Walker, JS, Kopp, RE, Shaw, TA, Cahill, N, Khan, NS, Barber, DC, Ashe, EL, Brain, MJ, Clear, JL, Corbett, DR and **Horton, BP.** 2021. Common Era sea-level budgets along the U.S. Atlantic coast. *Nature Communications*, 12(1): 1841. DOI: *https://doi.org/10.1038/s41467-021-22079-2*

Walton, WR. 1952. Techniques for recognition of living foraminifera. *Contribution from the Cushman Foundation the Foraminiferal Research*, 3(2): 56–60.

Wang, P and **Chappell, J.** 2001. Foraminifera as Holocene environmental indicators in the South Alligator River, Northern Australia. *Quaternary International*, 83–85: 47–62. DOI: *https://doi.org/10.1016/S1040-6182(01)00030-1*

Watcham, EP, Shennan, I and **Barlow, NLM.** 2013. Scale considerations in using diatoms as indicators of sea-level change: lessons from Alaska. *Journal of Quaternary Science*, 28(2): 165–179. DOI: *https://doi.org/10.1002/jqs.2592*

Wilson, GP and **Lamb, AL.** 2012. An assessment of the utility of regional diatom-based tidal-level transfer functions. *Journal of Quaternary Science*, 27(4): 360–370. DOI: *https://doi.org/10.1002/jqs.1553*

Woodroffe, SA. 2005. Intertidal mangrove foraminifera from the central Great Barrier Reef shelf, Australia: implications for sea-level reconstruction. *The Journal of Foraminiferal Research*, 35(3): 259–270. DOI: *https://doi.org/10.2113/35.3.259*

Woodroffe, SA. 2009. Recognising subtidal foraminiferal assemblages: implications for quantitative sea-level reconstructions using a foraminifera-based transfer function. *Journal of Quaternary Science*, 24(3): 215–223. DOI: *https://doi.org/10.1002/jqs.1230*

Woodroffe, SA and **Long, AJ.** 2010. Reconstructing recent relative sea-level changes in West Greenland: Local diatom-based transfer functions are superior to regional models. *Quaternary International*, 221(1): 91–103. DOI: *https://doi.org/10.1016/j.quaint.2009.06.005*

Wright, AJ, Edwards, RJ and **van de Plassche, O.** 2011. Reassessing transfer-function performance in sea-level reconstruction based on benthic salt-marsh foraminifera from the Atlantic coast of NE North America. *Marine Micropaleontology*, 81(1–2): 43–62. DOI: *https://doi.org/10.1016/j.marmicro.2011.07.003*

Zong, Y and **Horton, BP.** 1999. Diatom-based tidal-level transfer functions as an aid in reconstructing Quaternary history of sea-level movements in the UK. *Journal of Quaternary Science*, 14(2): 153–167. DOI: *https://doi.org/10.1002/(SICI)1099-1417(199903)14:2<153::AID-JQS425>3.0.CO;2-6*